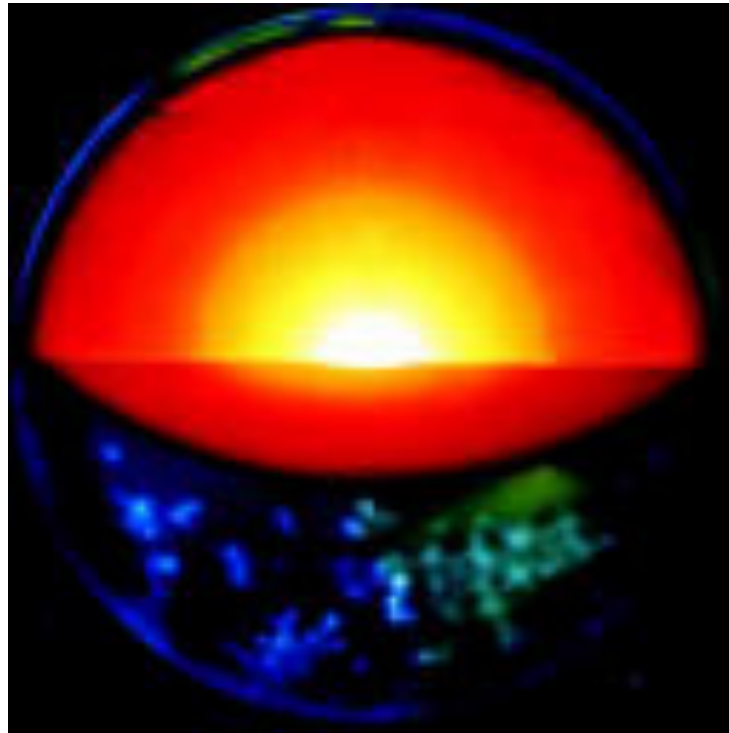
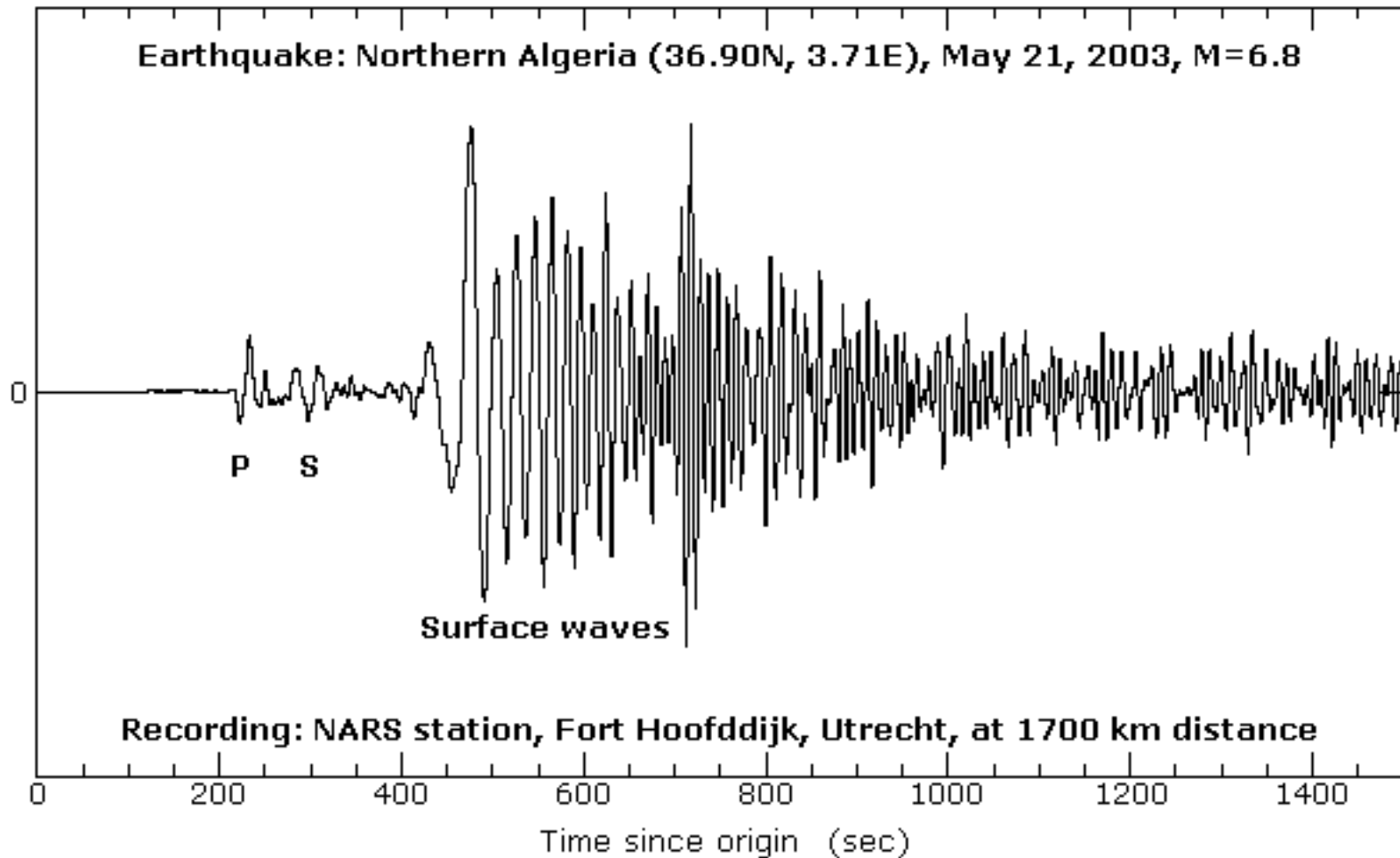
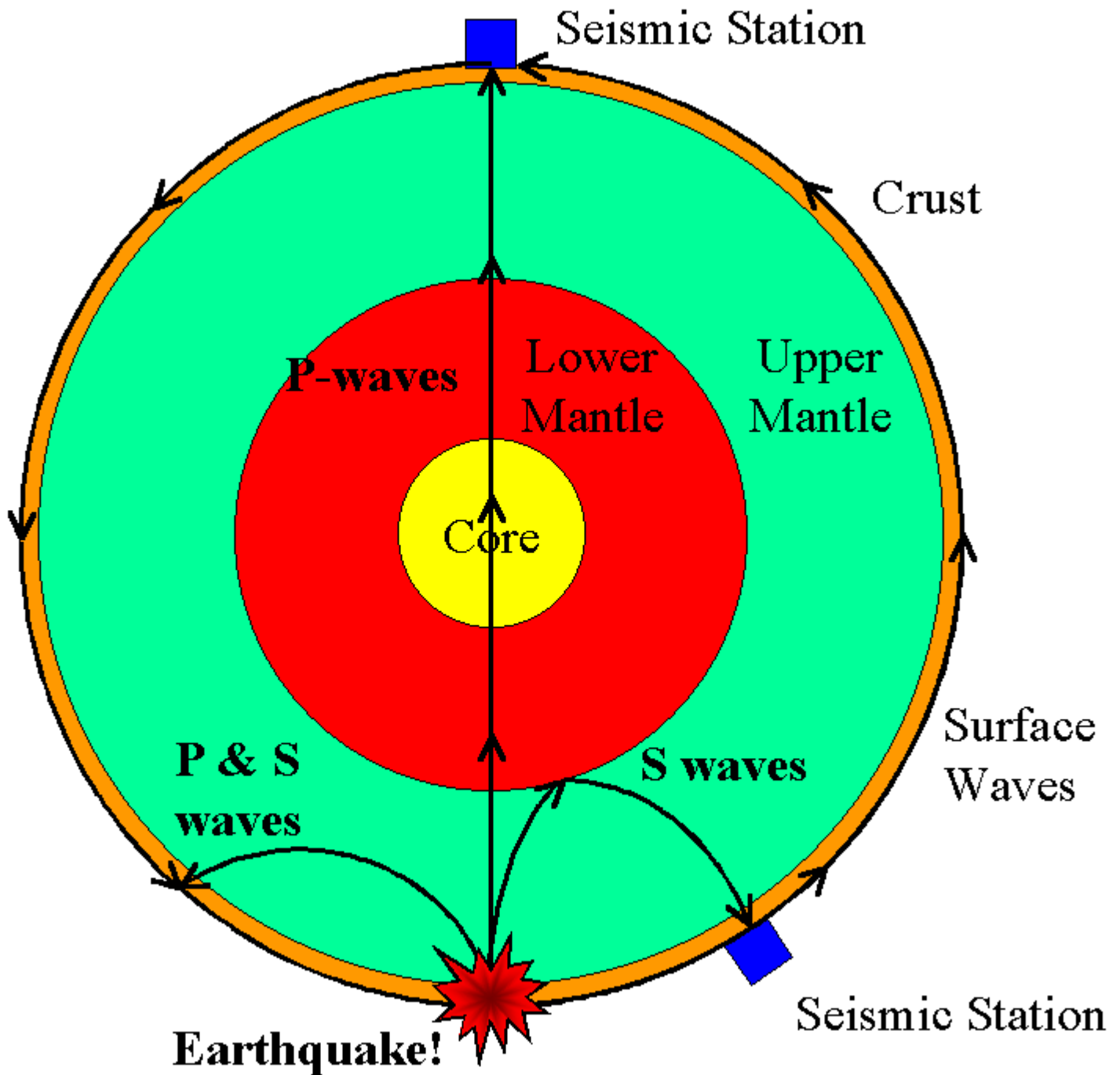


# Earth's internal structure: a seismologist's view



# Types of waves used by seismologists





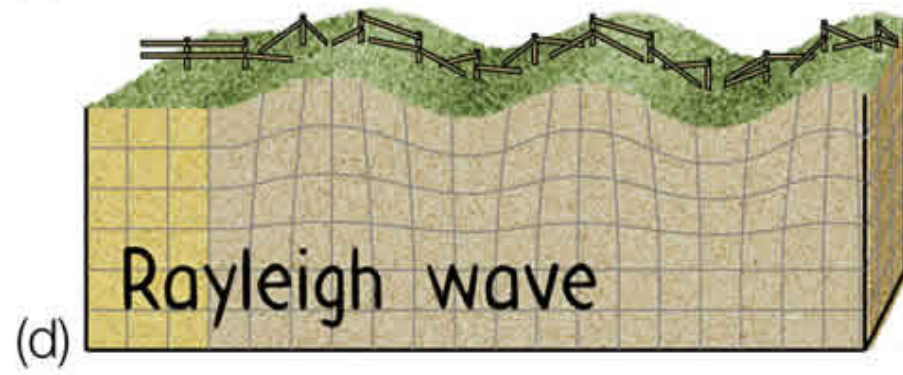
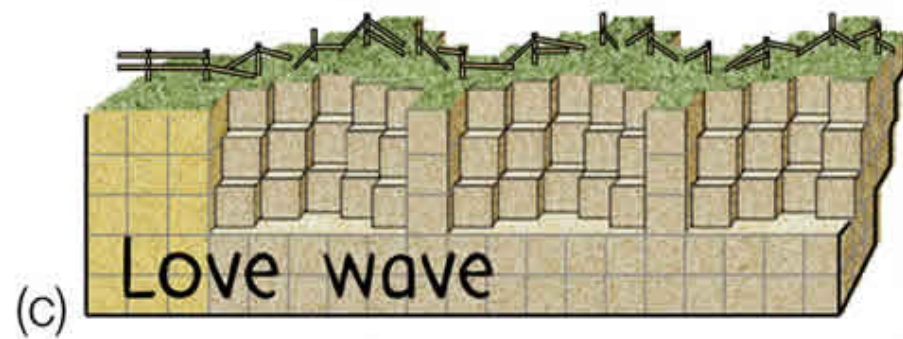
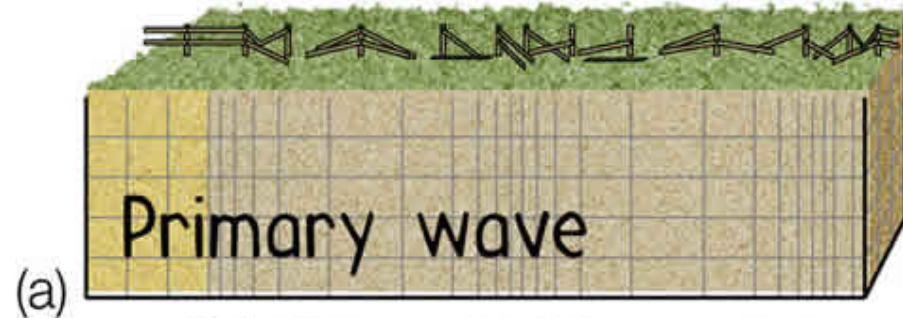


**Figure 2.9-7: Examples of the displacements for several spheroidal modes.**

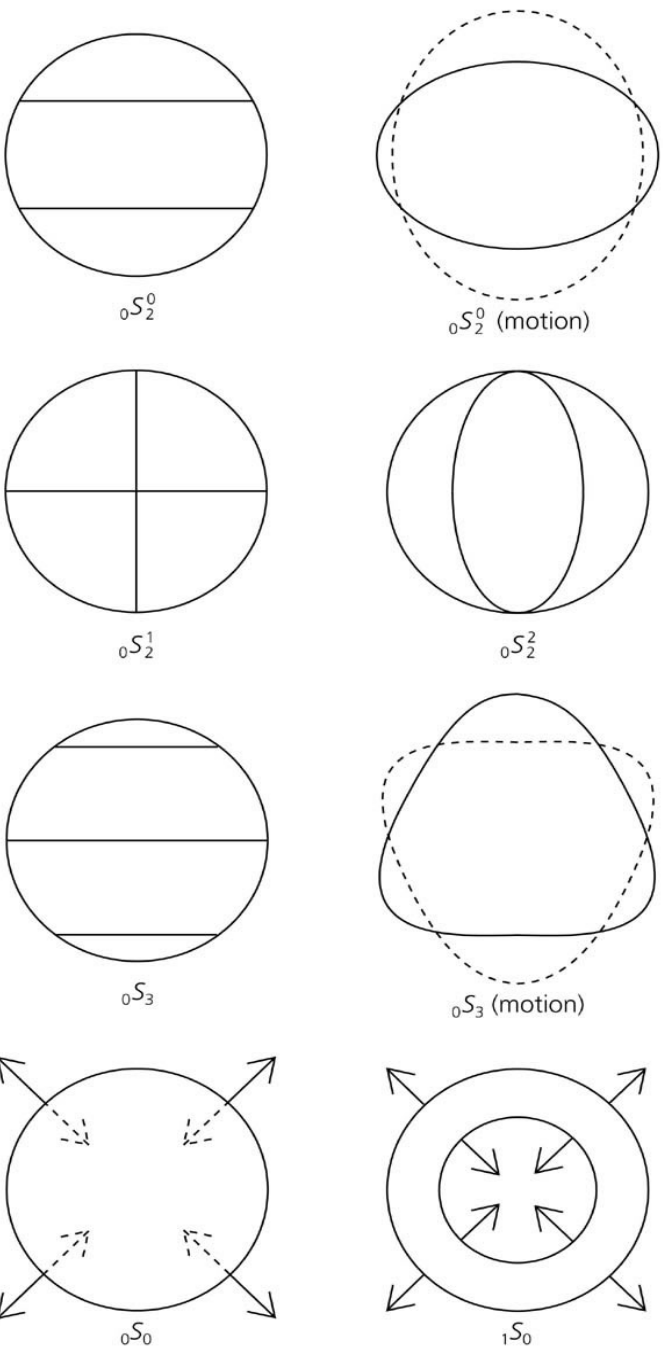
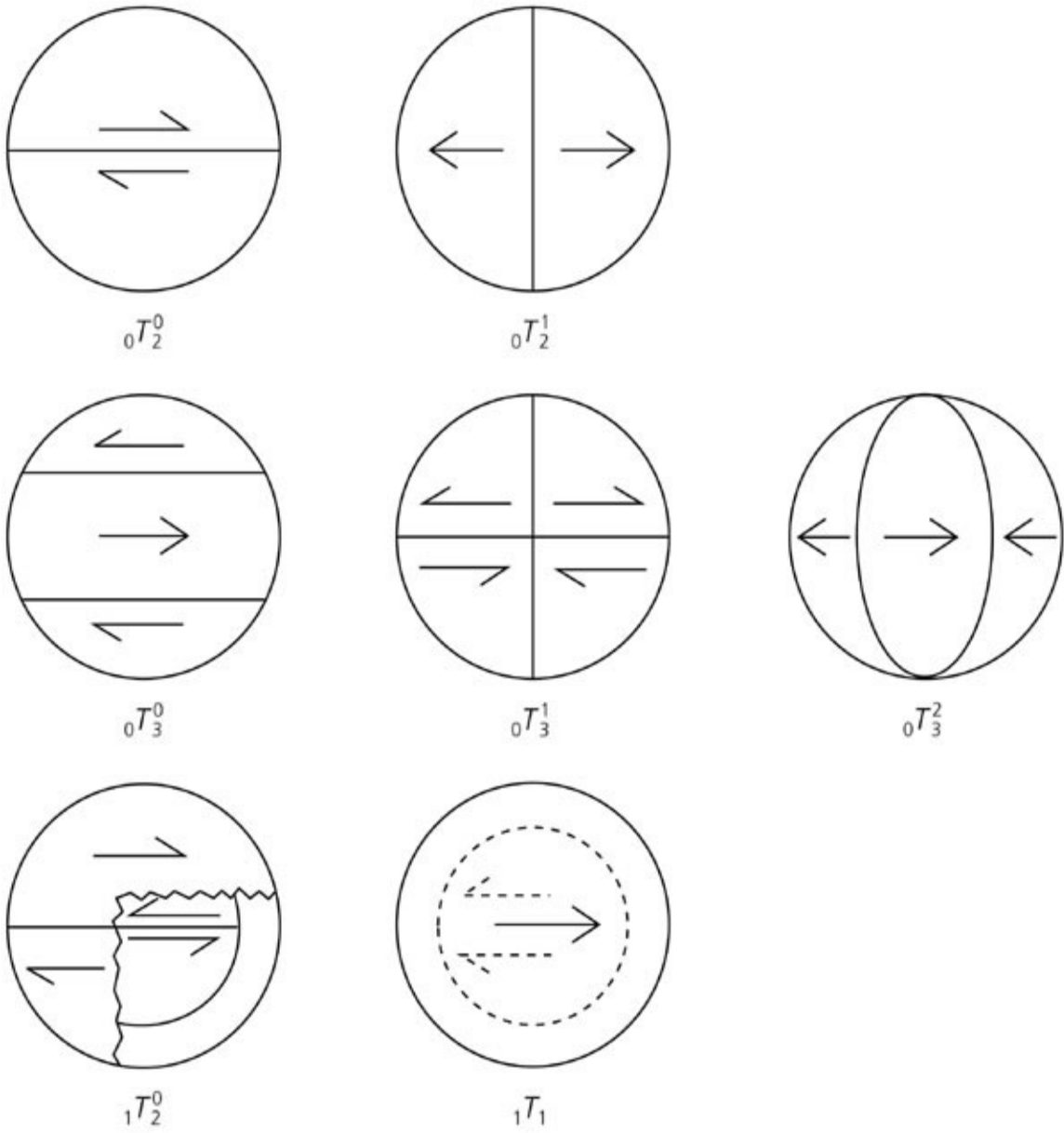


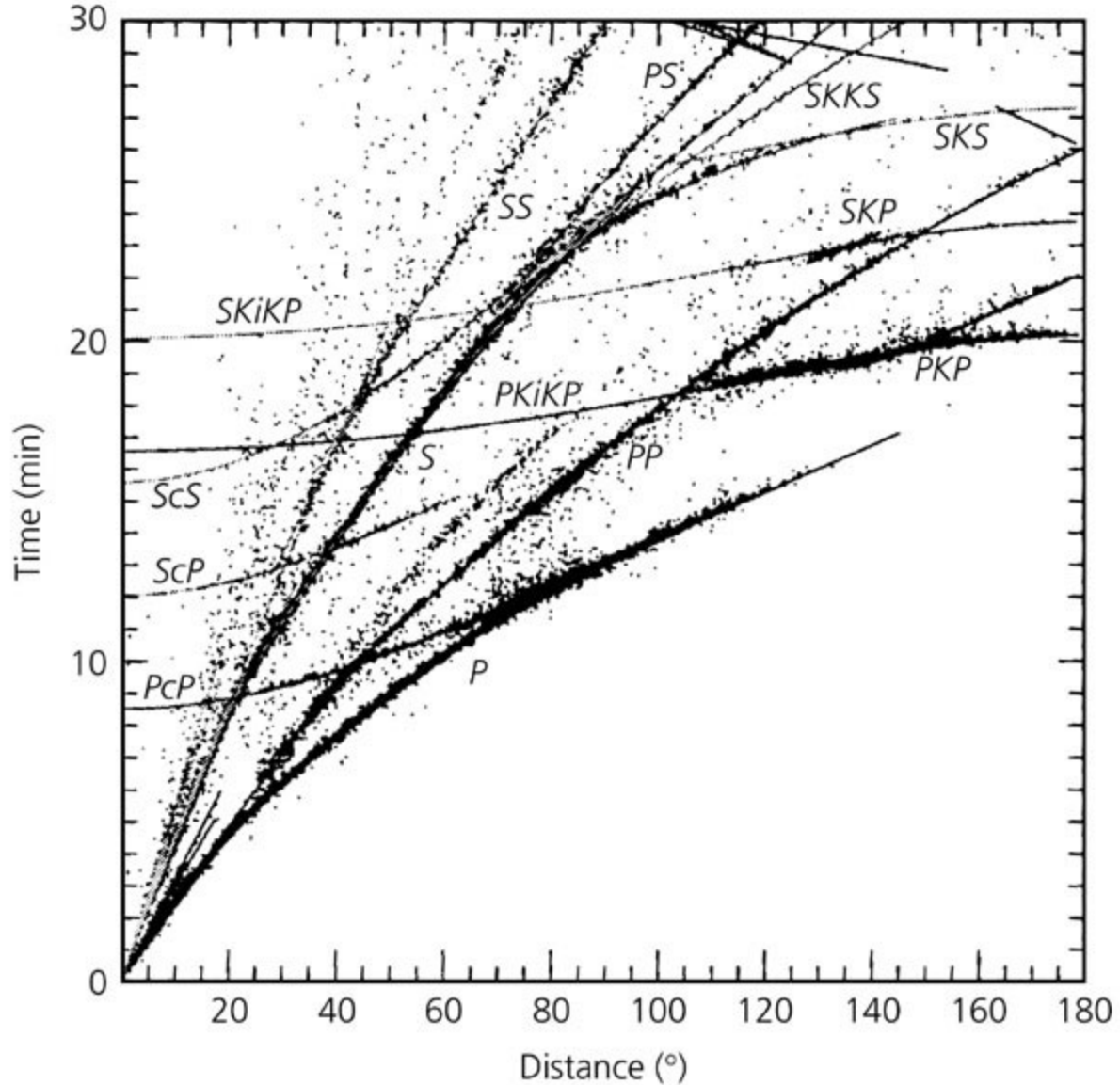
**Figure 2.9-6: Examples of the displacements for several torsional modes.**



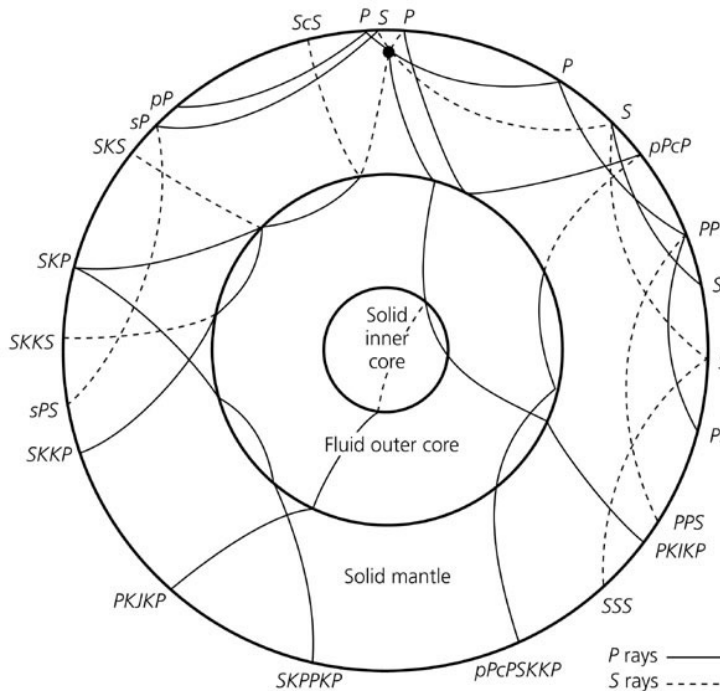
# Organizing the information

- Seismic travel times
- Dispersion curves
- Free oscillation frequencies

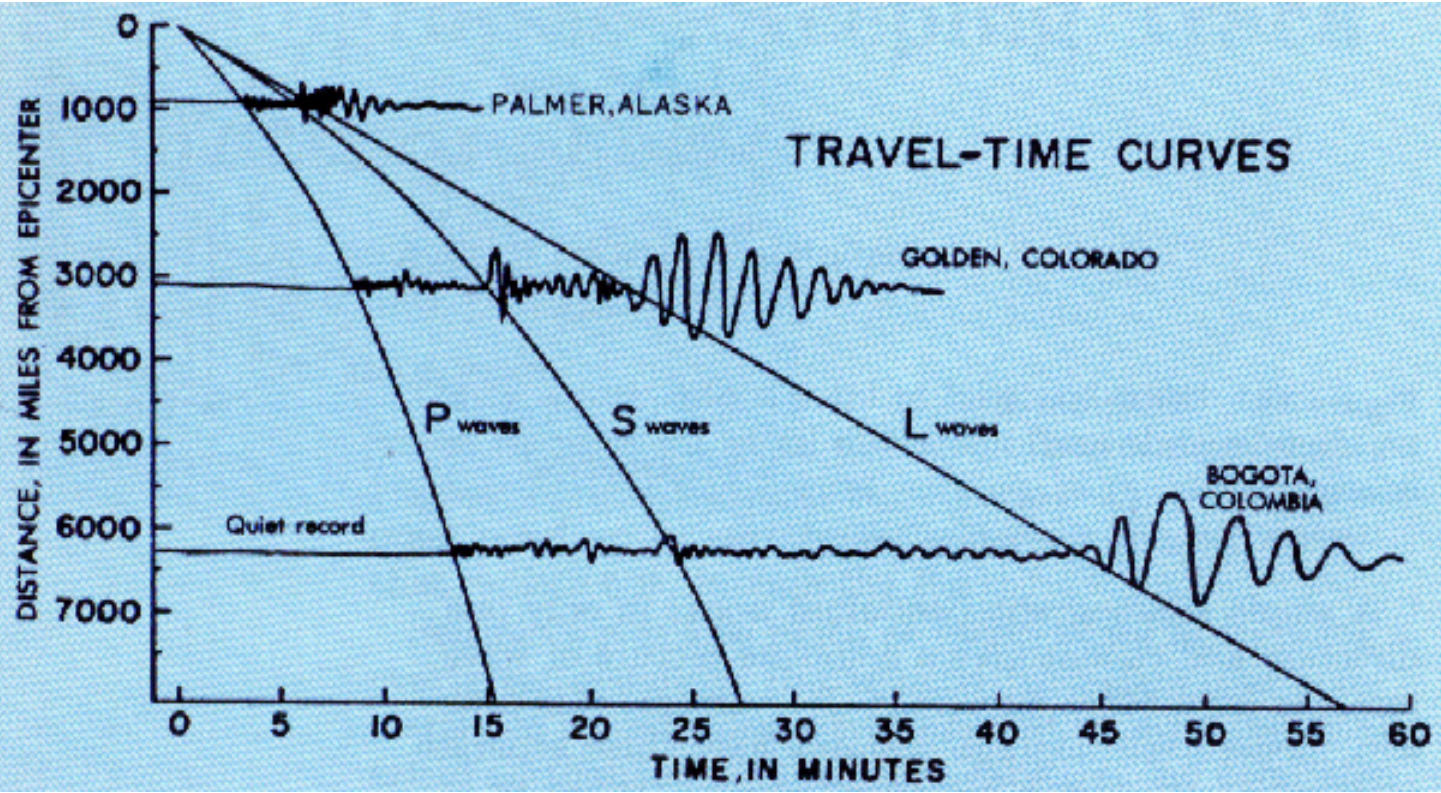
**Figure 3.5-3: Travel time data and curves for the IASP91 model.**



**Figure 3.5-5: Illustration of various body wave phases.**

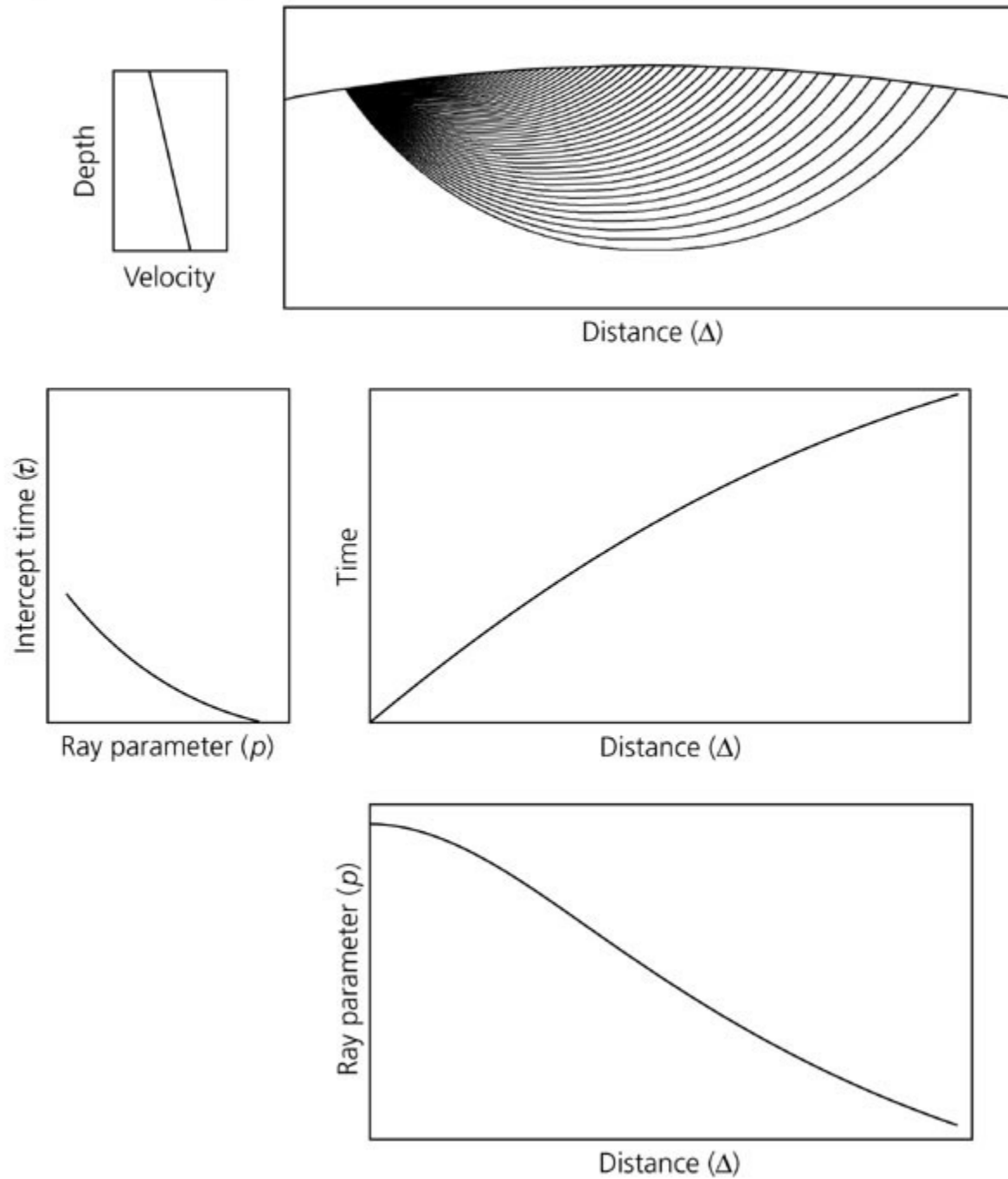




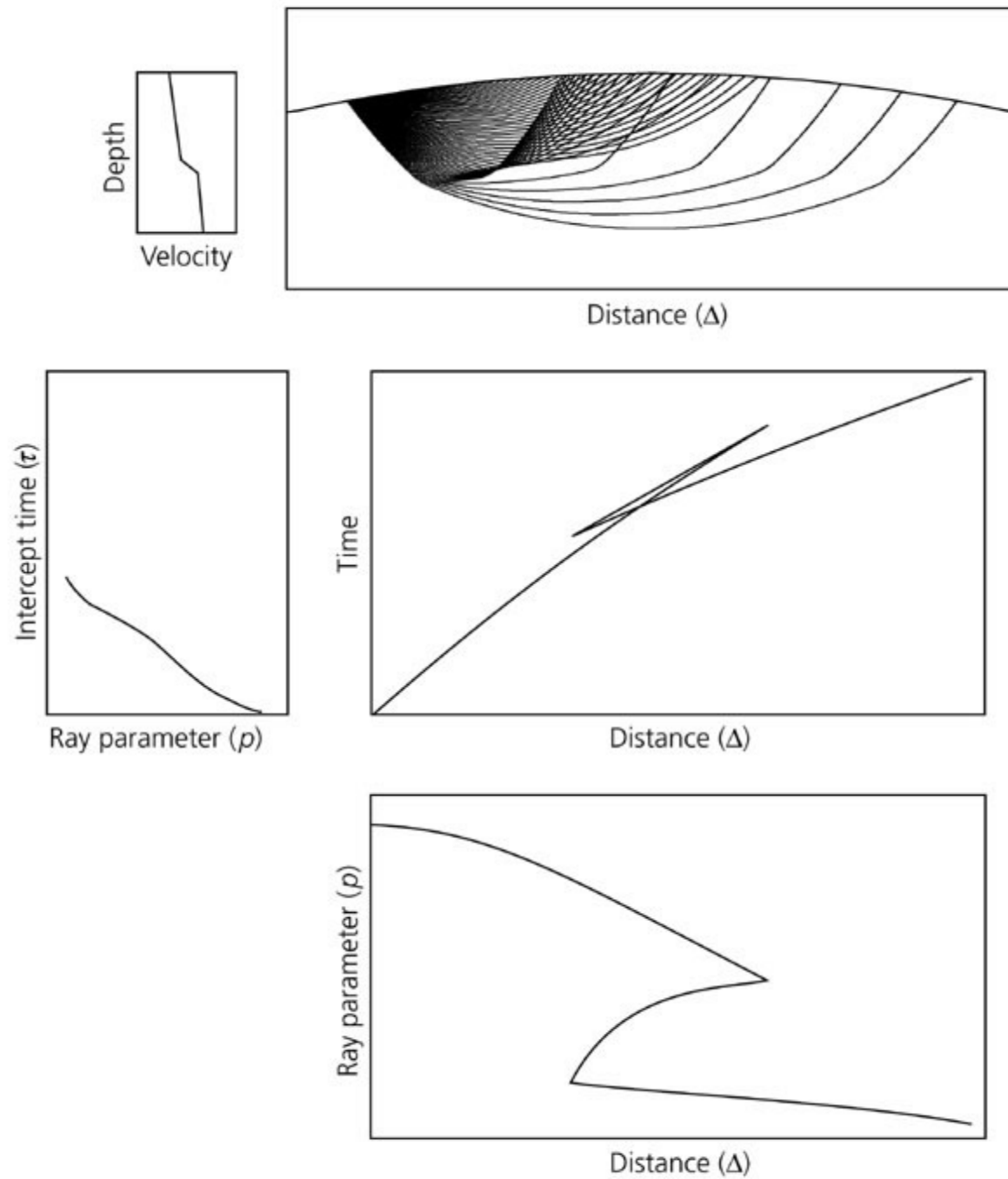




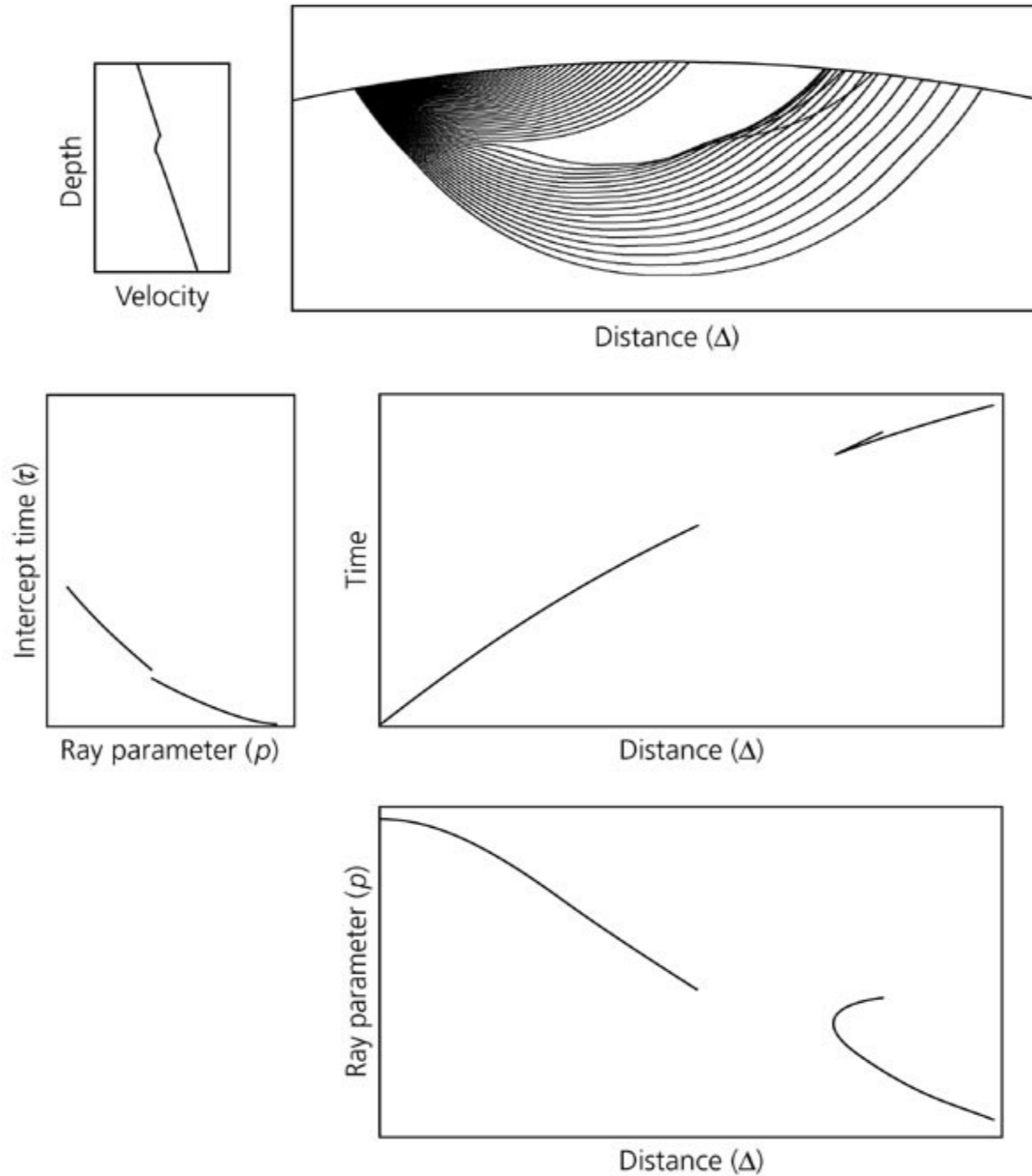
**Figure 3.4-5: Ray path effects for increasing velocity.**



**Figure 3.4-6: Ray path triplcation effects for a velocity increase.**



**Figure 3.4-7: Ray path shadow-zone effects for a velocity decrease.**



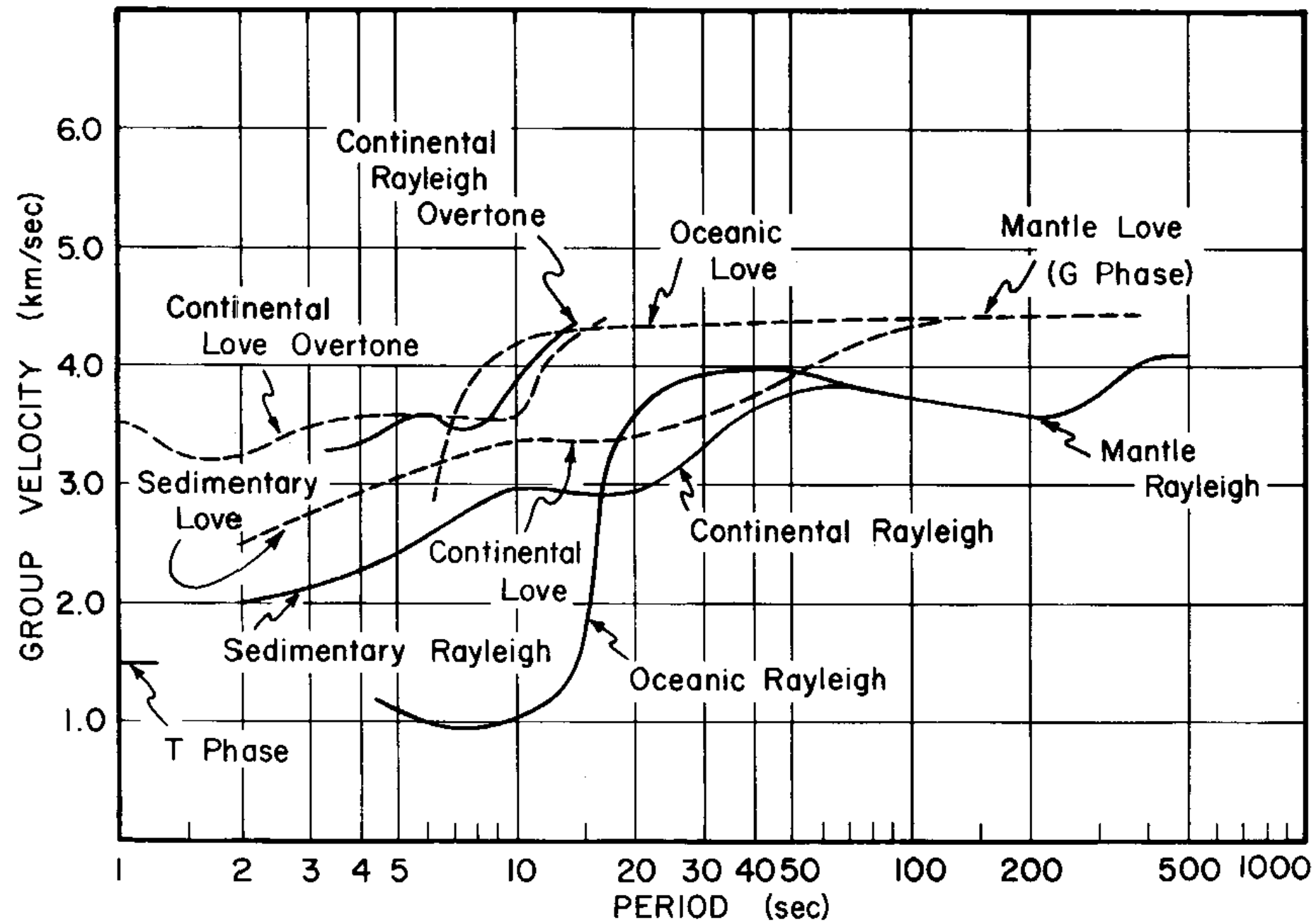
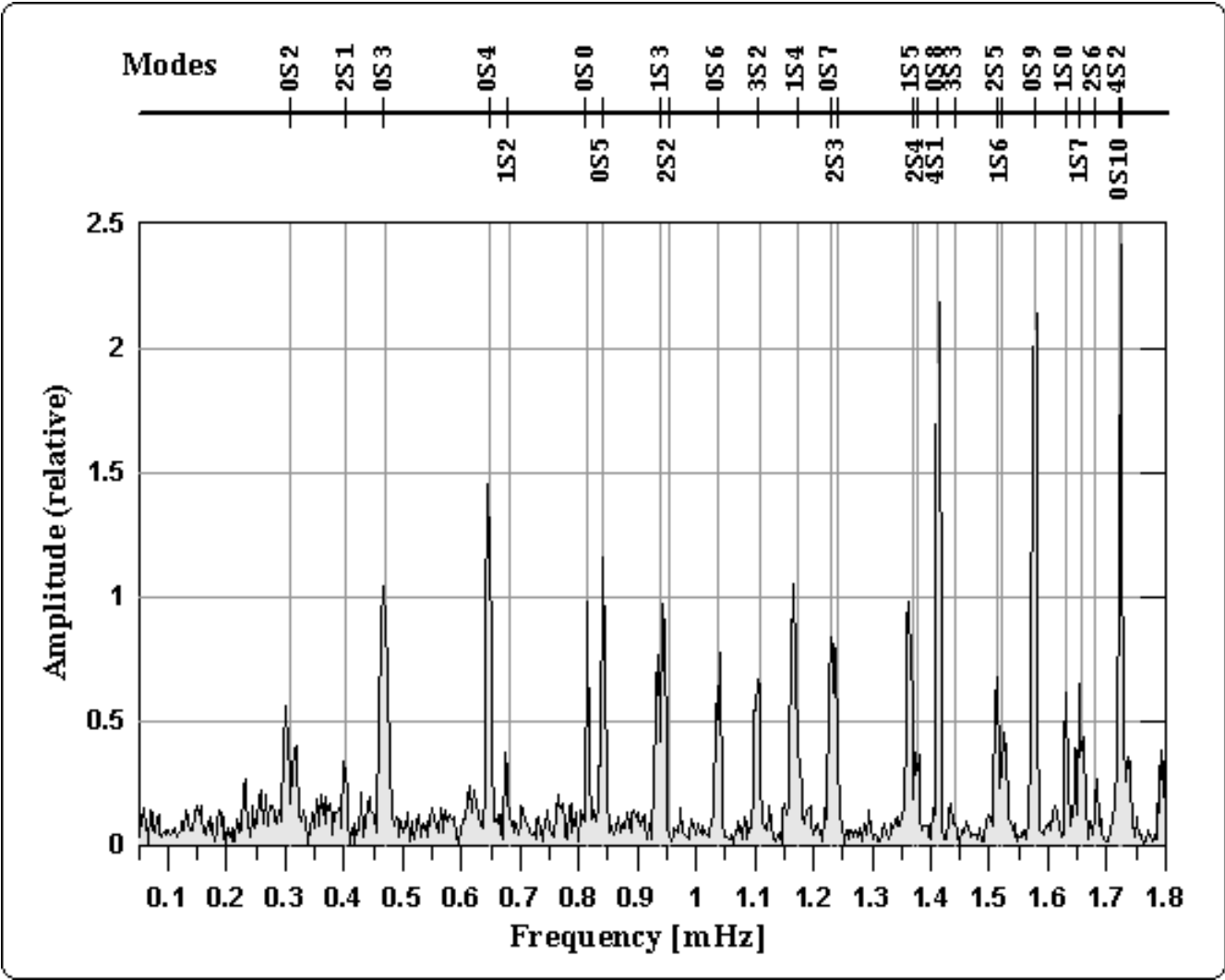
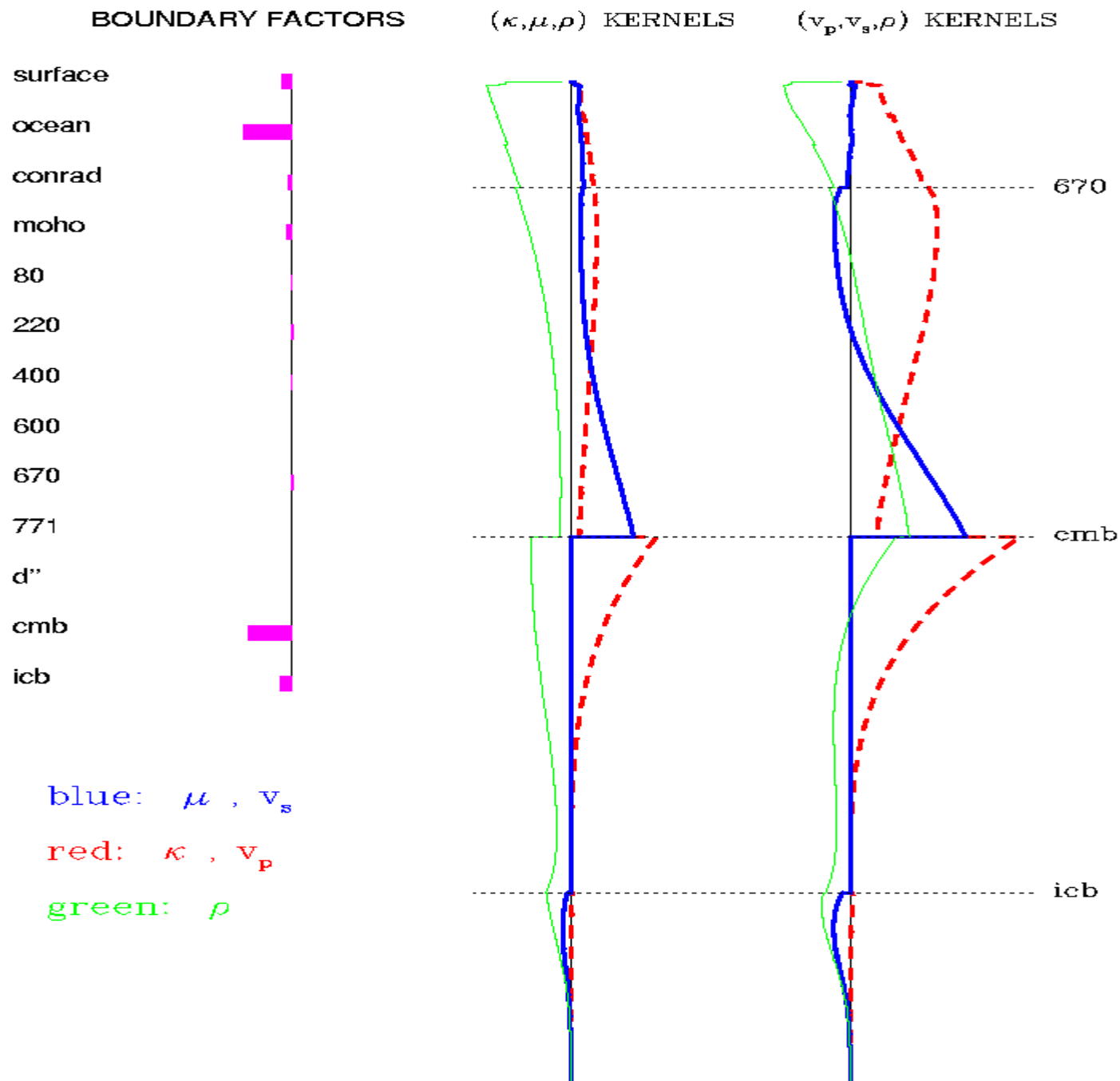


Figure 1.2.1b Composite of dispersion curves for surface waves.



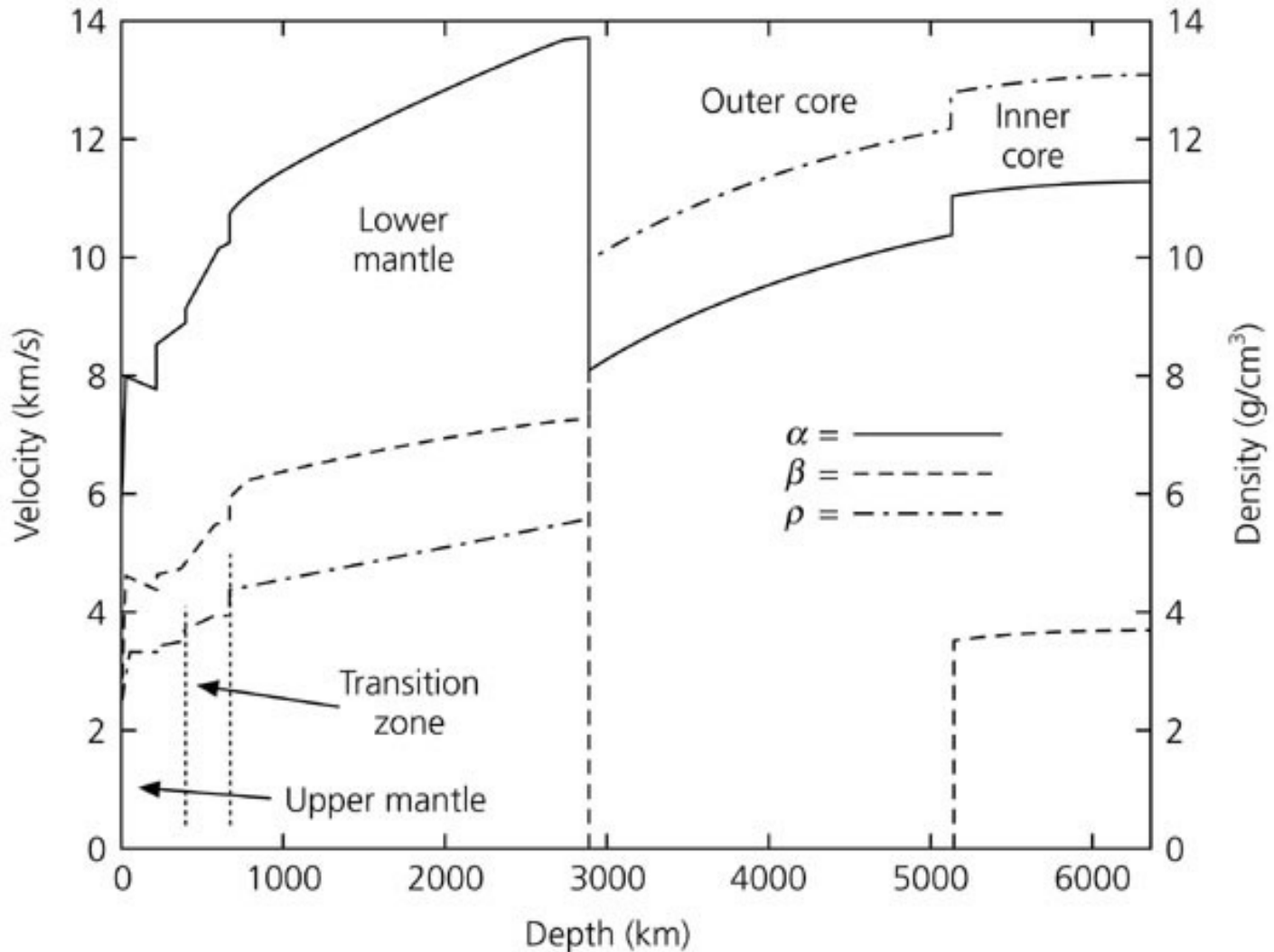
# CATAL/3s\_catal/3s2 KERNELS OF LOWEST DEGREE

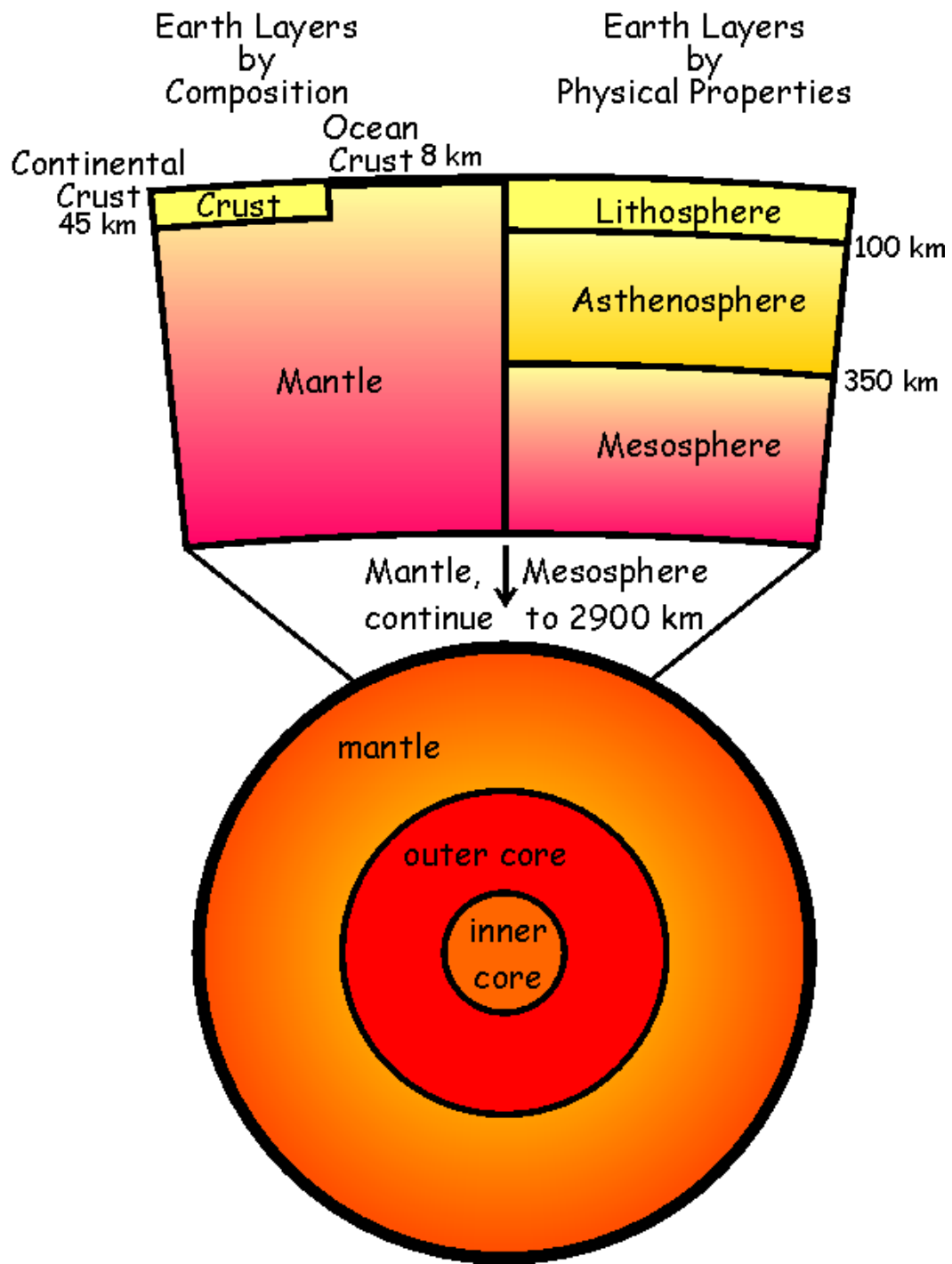




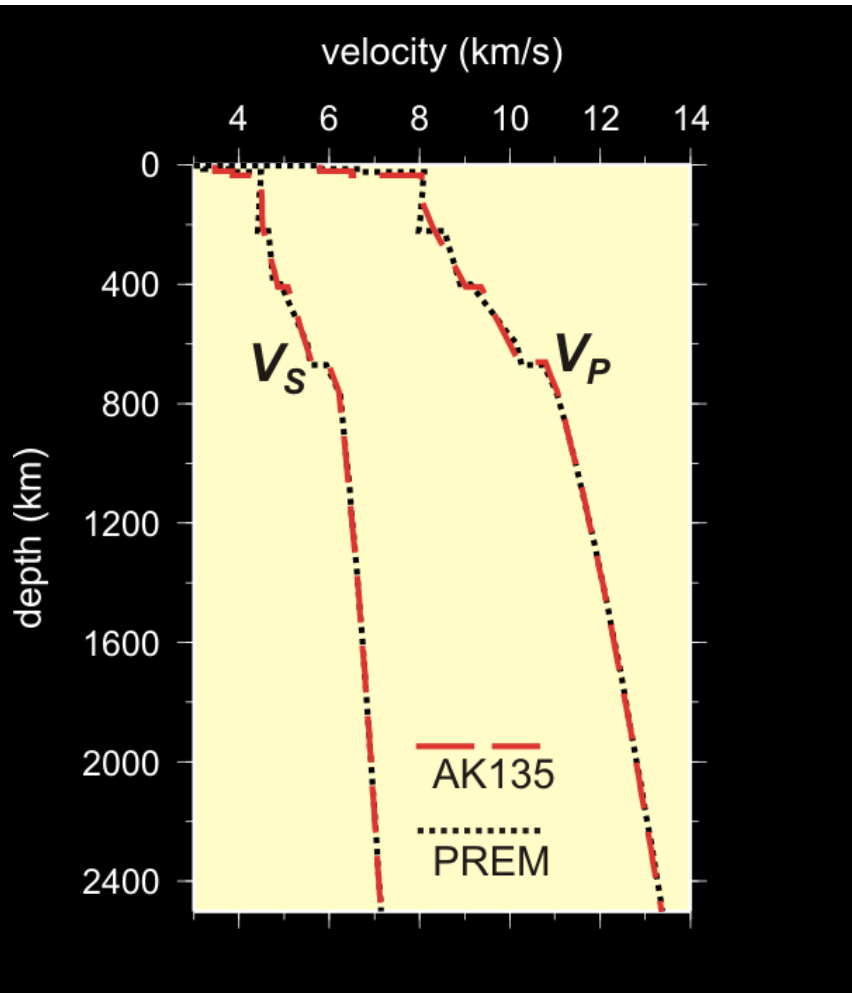
# Putting it all together

**Figure 3.8-4: Preliminary Reference Earth Model.**





# Mantle 1-D seismic structure summary



- Between 10-50 km have Mohorovicic discontinuity – this marks the CRUST/ MANTLE boundary
- At 50-200 km have a LOW VELOCITY ZONE – particularly under oceans and younger continents

# The crust

Figure 3.2-1: Ray paths for a layer over a halfspace.

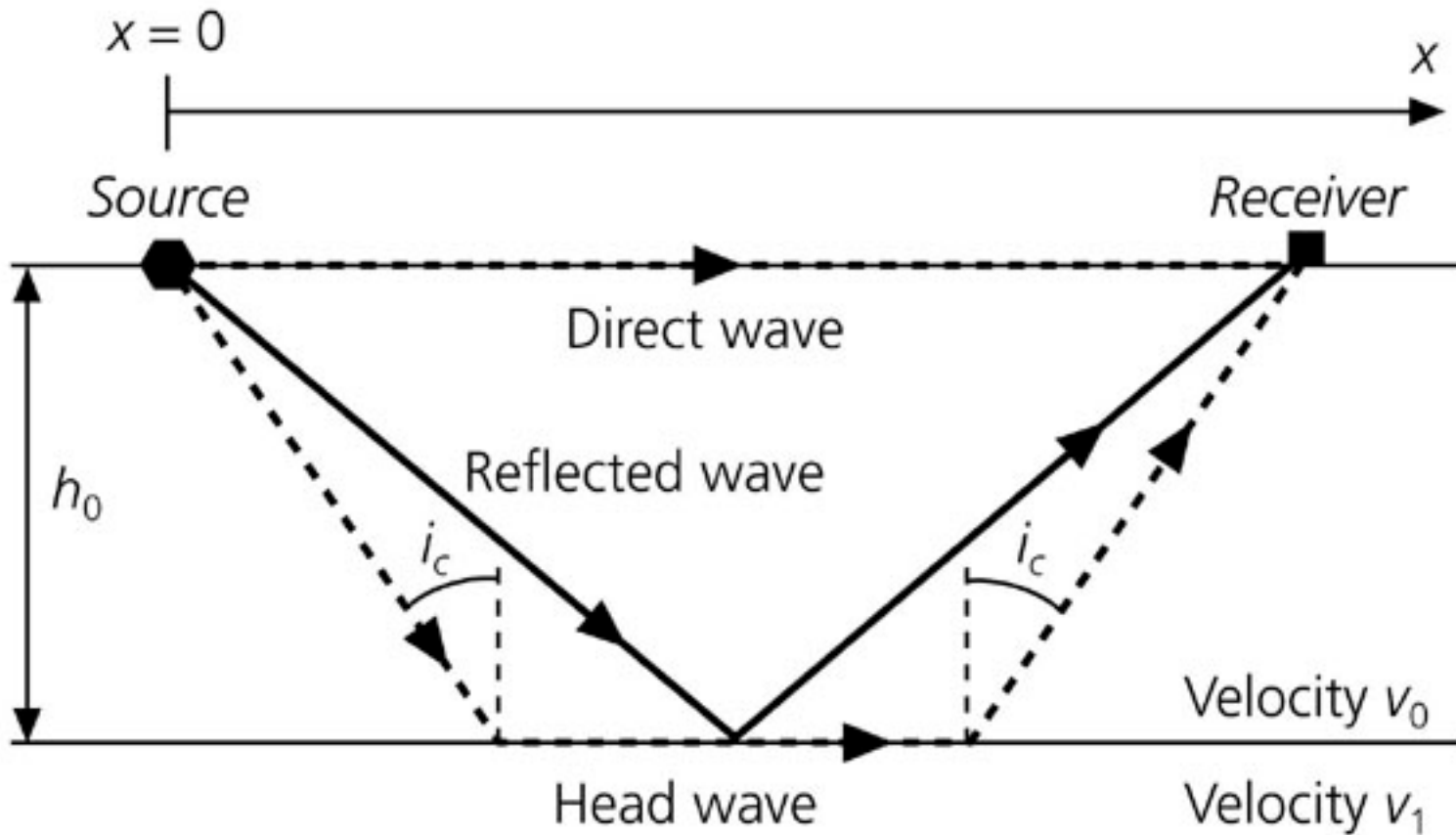
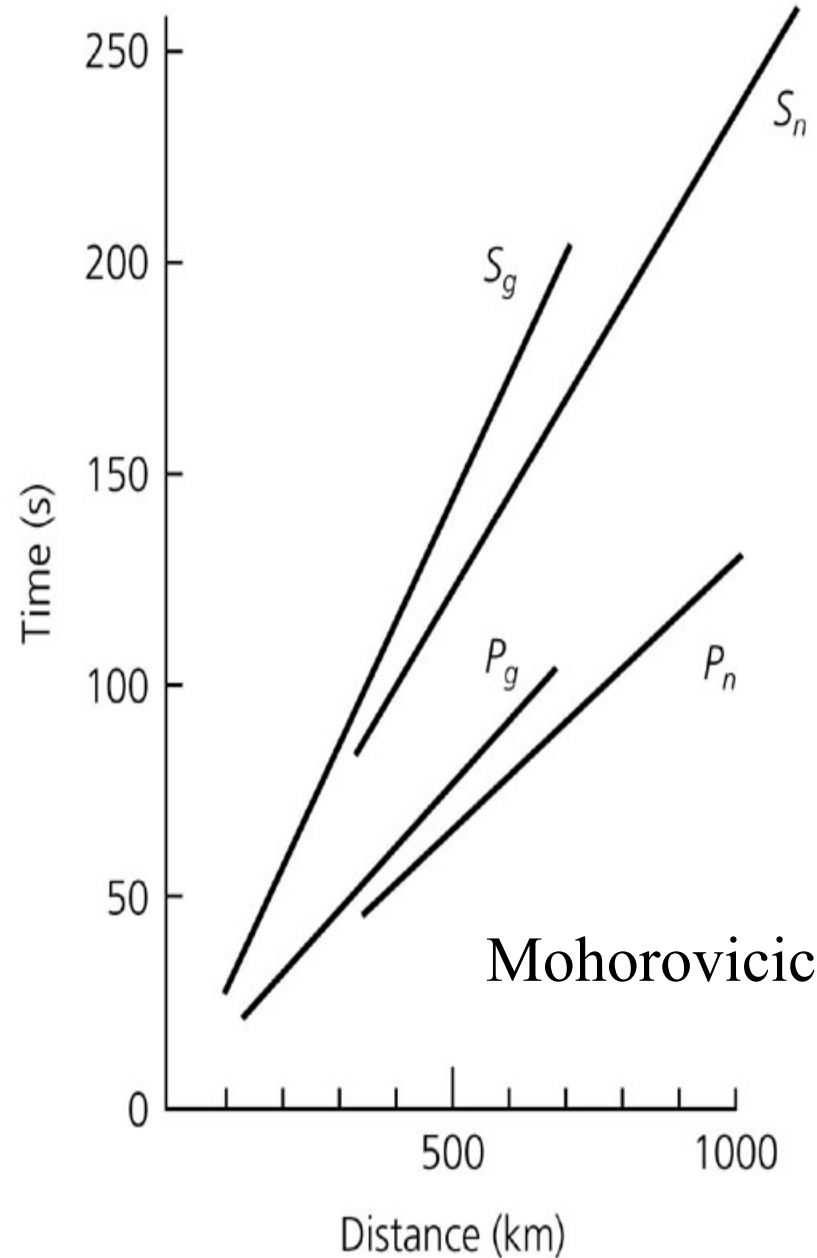
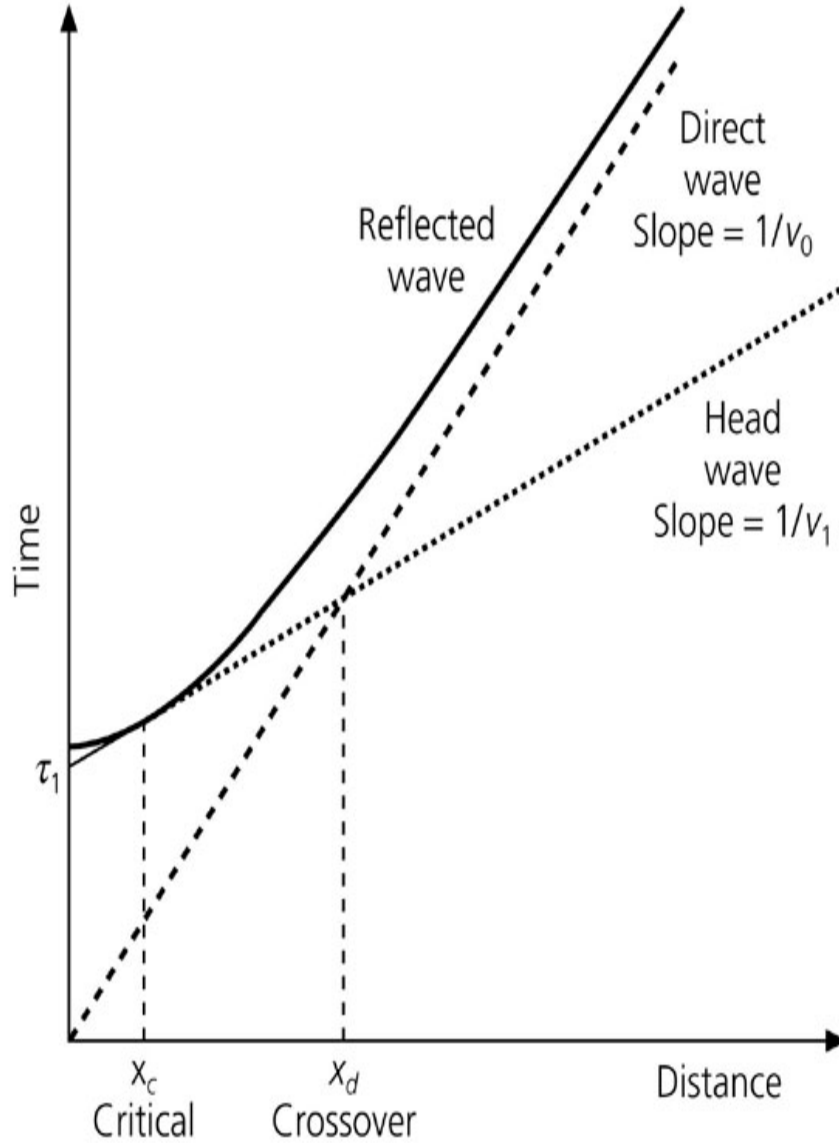


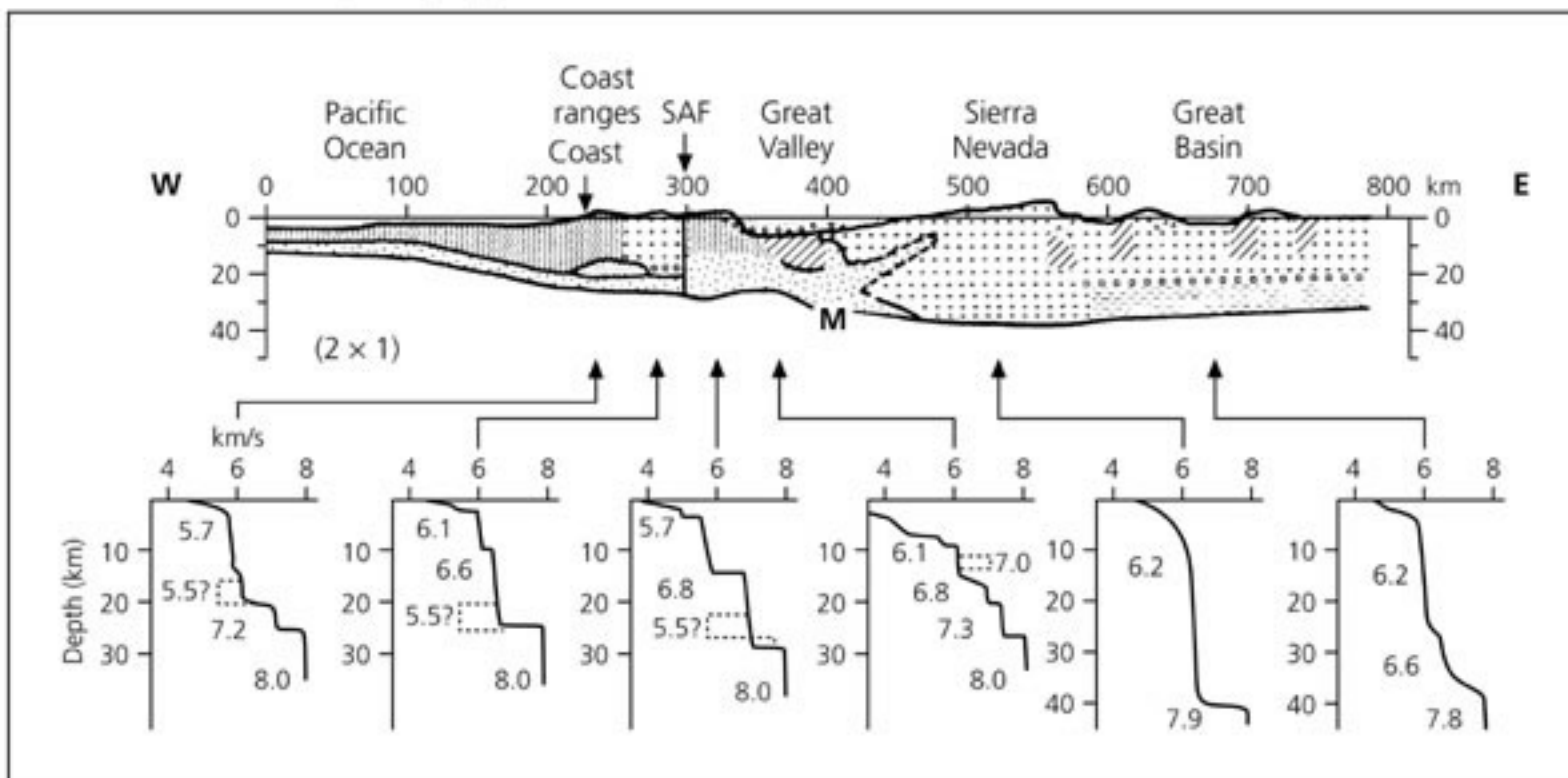
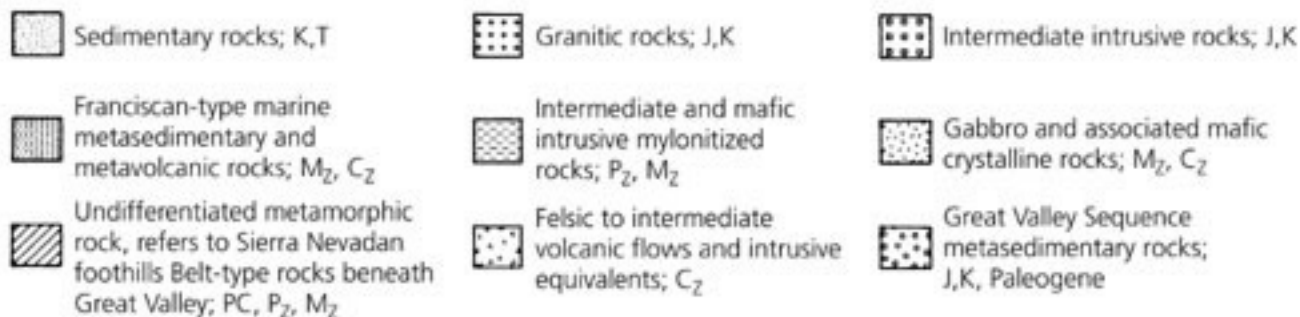
Figure 3.2-5: Example of seismograms from a refraction profile.

Figure 3.2-2: Travel time curve for rays in a layer over a halfspace.



Mohorovicic 1909

**Figure 3.2-17: Crustal models for the western U.S.**





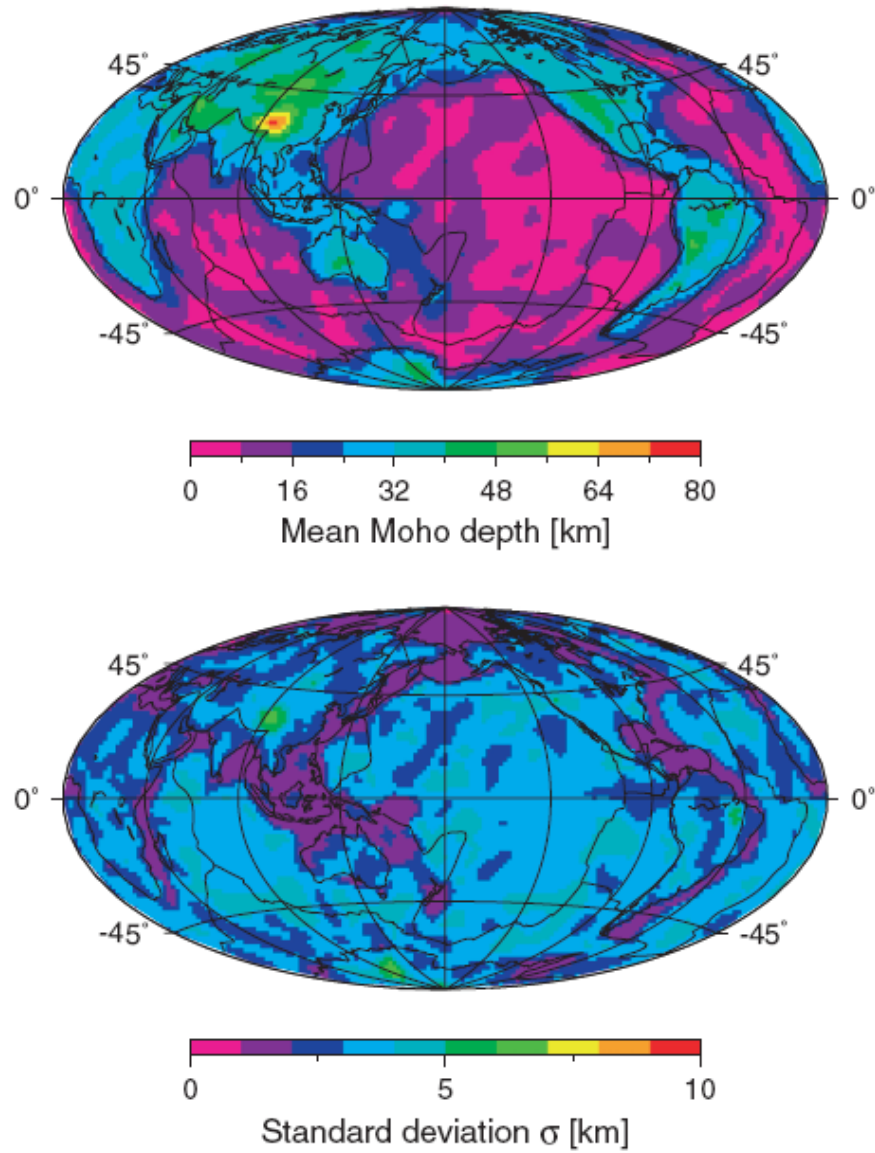


**Figure 12.** Global Moho depth map as a result of the joint inversion. (top) mean Moho depth [km]; (bottom) standard deviation  $\sigma$  [km], both extracted from the output of a MDN network.

# The lithosphere

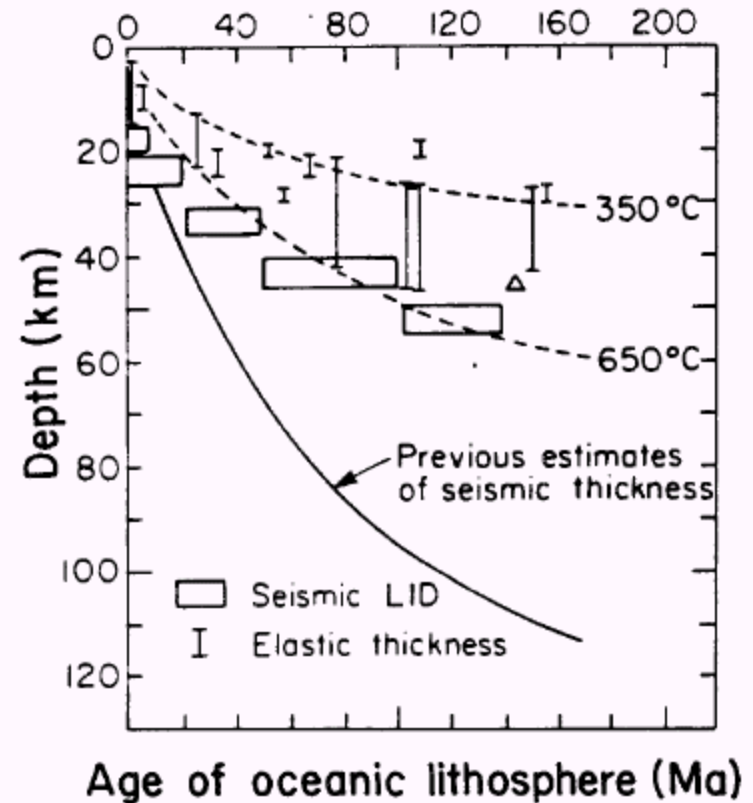


**FIGURE 3-2**

The thickness of the lithosphere as determined from flexural loading studies and surface waves. The upper edges of the open boxes gives the thickness of the seismic LID (high-velocity layer, or seismic lithosphere). The lower edge gives the thickness of the mantle LID plus the oceanic crust (Regan and Anderson, 1984). The triangle is a refraction measurement of oceanic seismic lithosphere thickness (Shimamura and others, 1977). The LID under continental shields is about 150 km thick (see Figure 3-4).

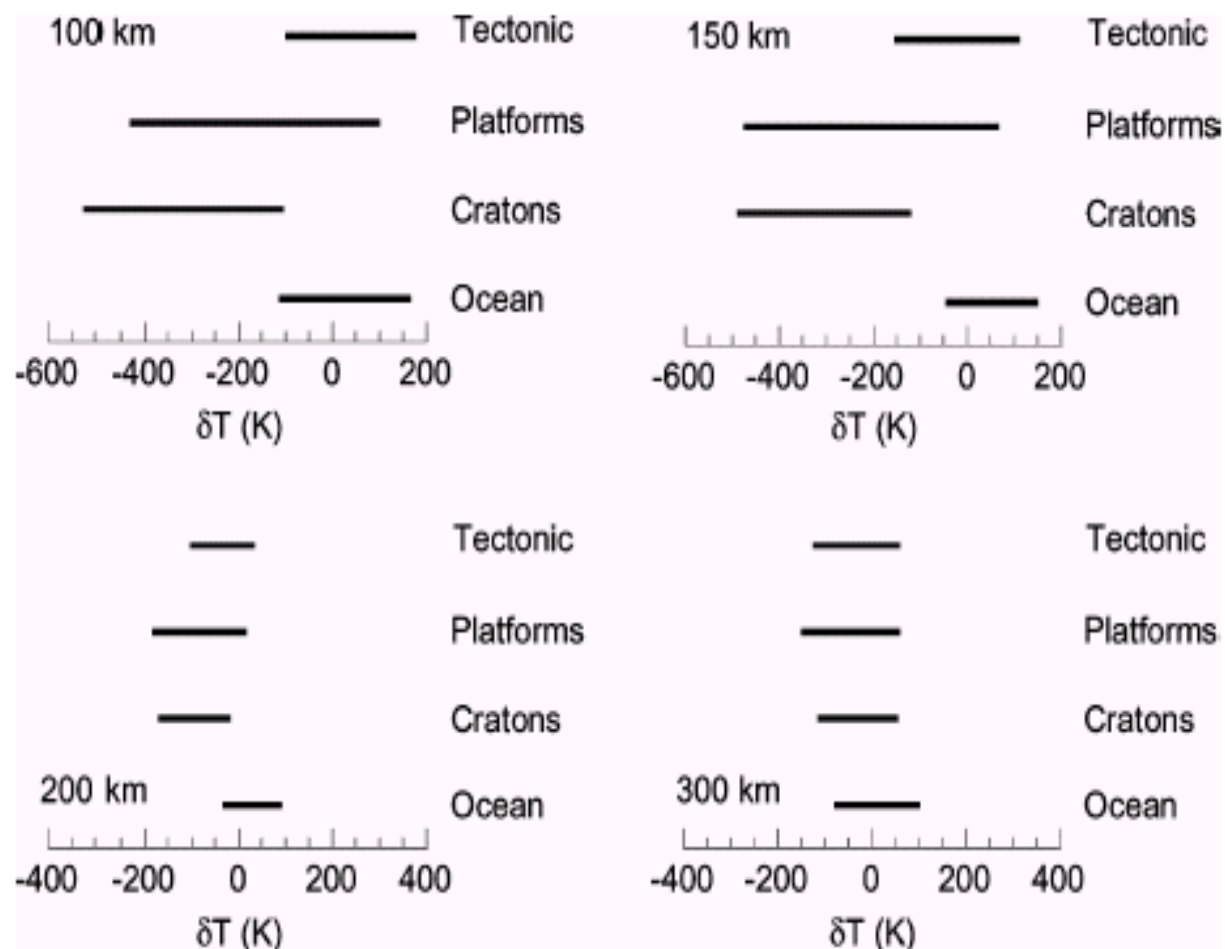


Fig. 5. Statistics on the distribution of temperature anomalies for several regions and depths (indicated on each plot). The tectonic regions are delimited following the model 3SMAC (Nataf and Ricard, 1996).

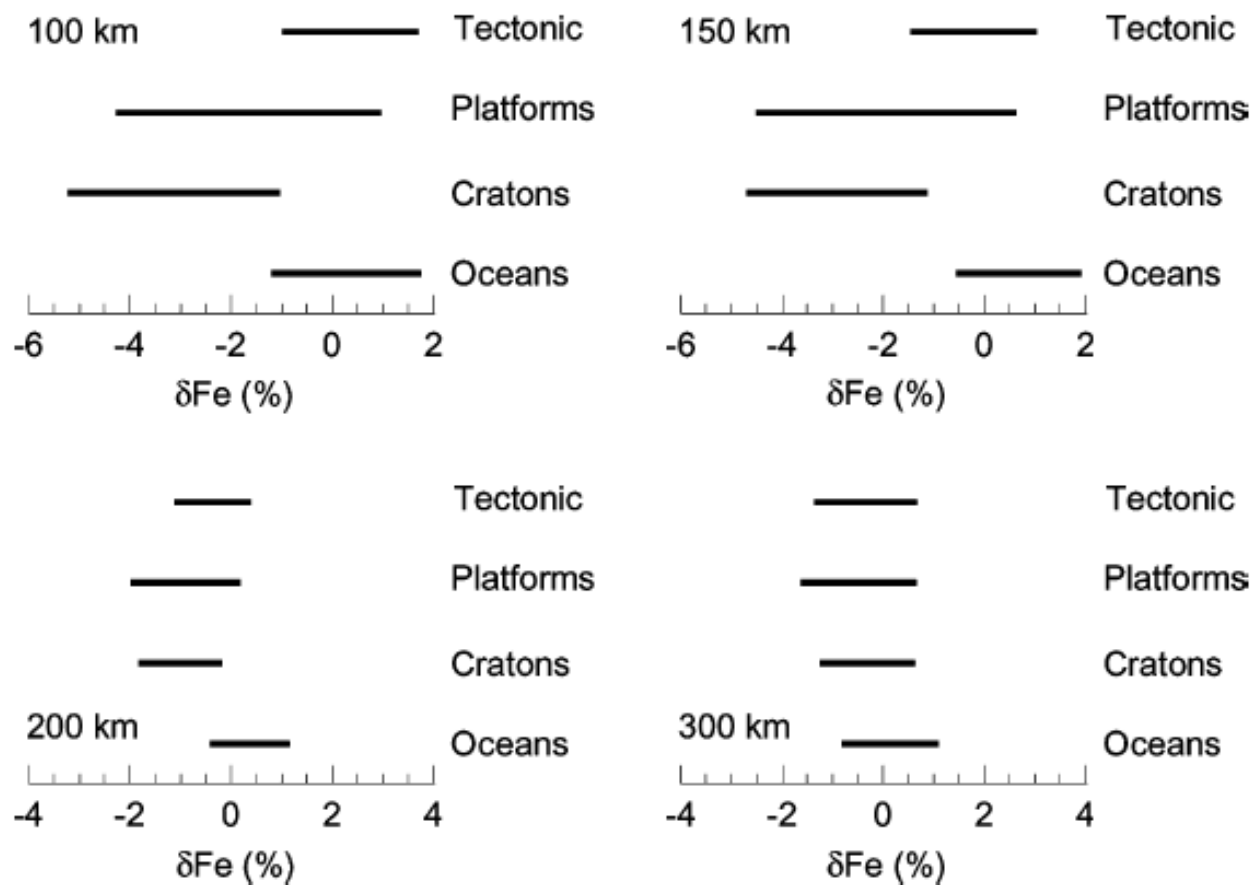
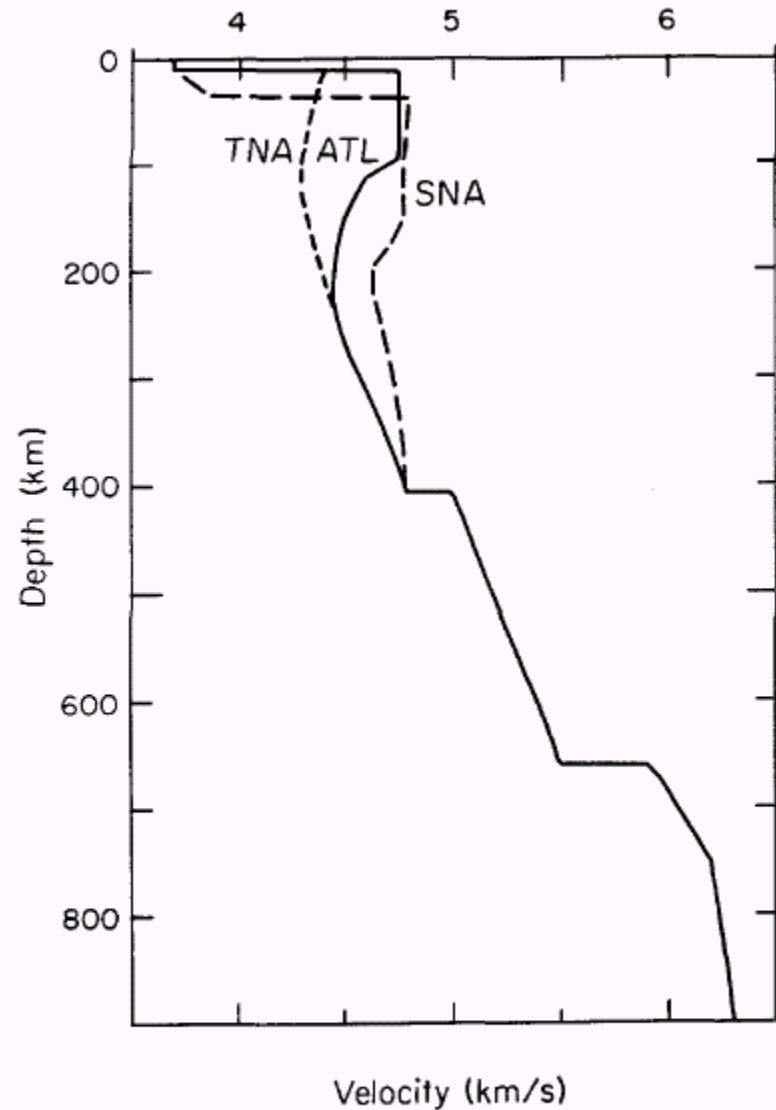


Fig. 6. Statistics on the distribution of iron anomalies for several regions and depths (indicated on each plot). The tectonic regions are delimited following the model 3SMAC (Nataf and Ricard, 1996).

# The asthenosphere



**FIGURE 3-4**

High-resolution shear-wave velocity profiles for various tectonic provinces; TNA is tectonic North America, SNA is shield North America, ATL is north Atlantic (after Grand and Helmberger, 1984).

# Compositional interpretation of 1-D seismic profiles

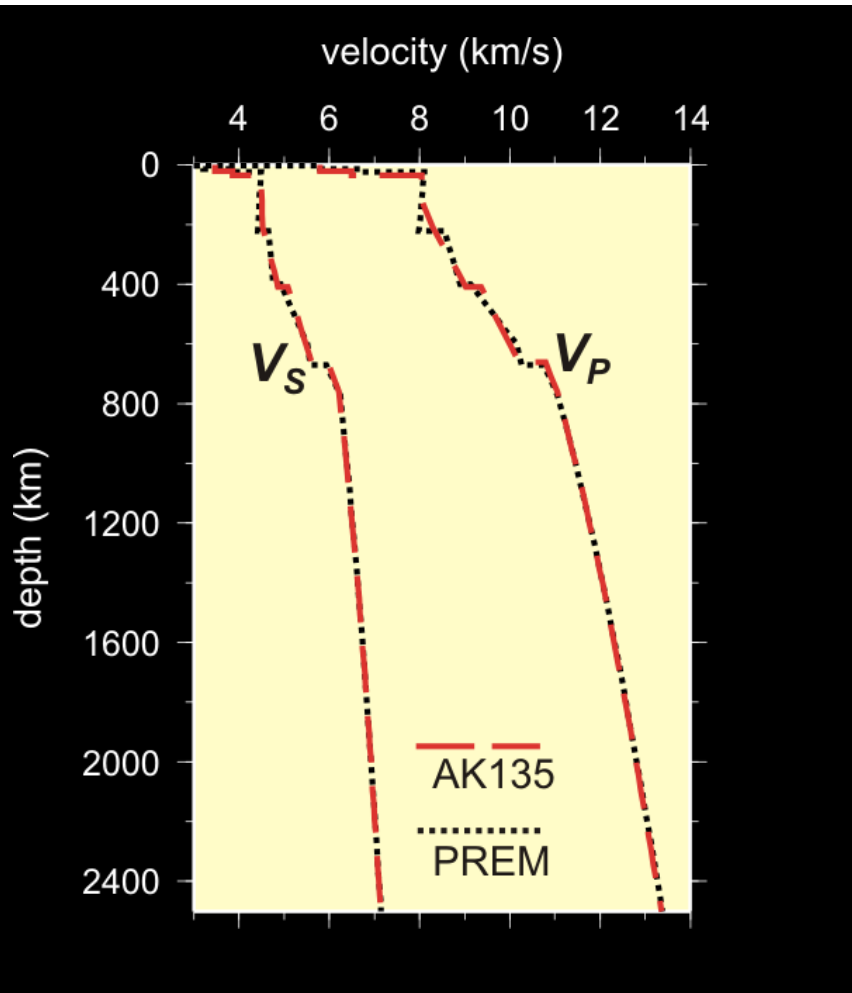
Seismic discontinuities and velocity gradients can arise from

- A chemical change (e.g. the Moho)
- A phase change  
(reorganisation of atoms into a different crystalline structure)

The relative roles of phase changes and chemical changes provide a major challenge in interpreting seismology.



# Mantle 1-D seismic structure summary



- Several seismological methods indicate a discontinuity near **220 km** depth.
- Although present on PREM, it is now generally accepted ***not to be a global feature***
- Sometimes called the “Lehmann discontinuity” after Inge Lehmann

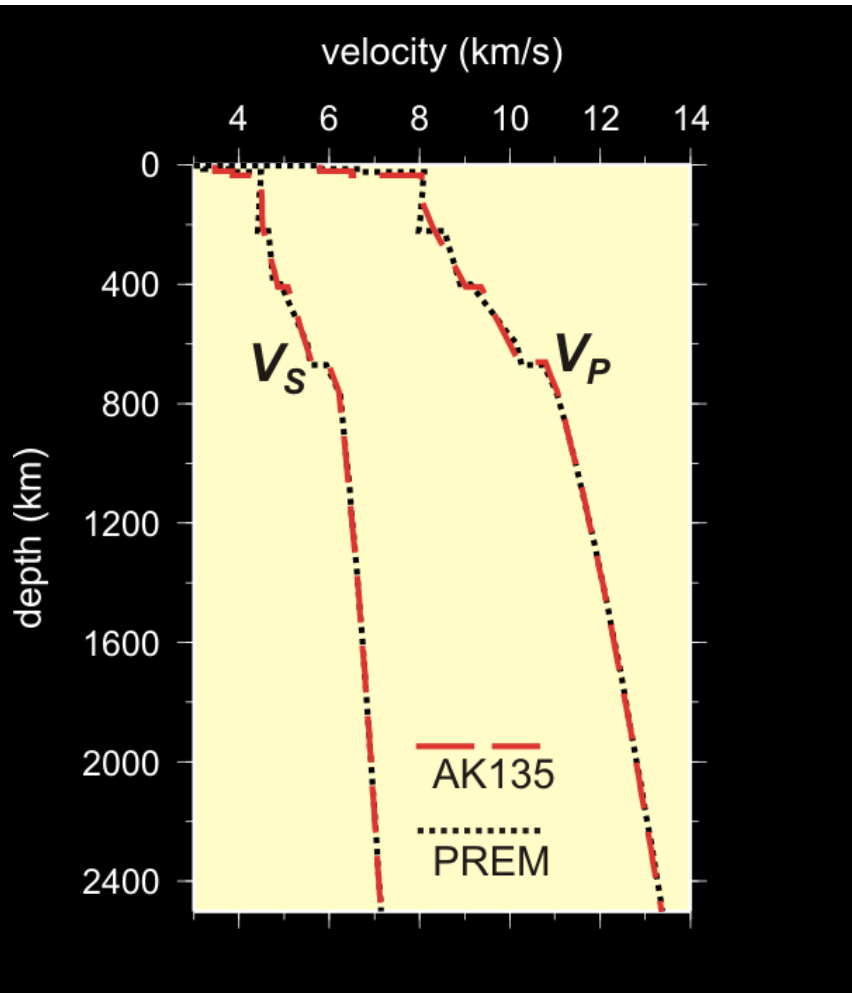
# NB: The 220-km Lehmann Discontinuity

Not global in character!

May reflect local anisotropy due to shearing of the asthenosphere

i.e. a *textural* rather than chemical or phase change

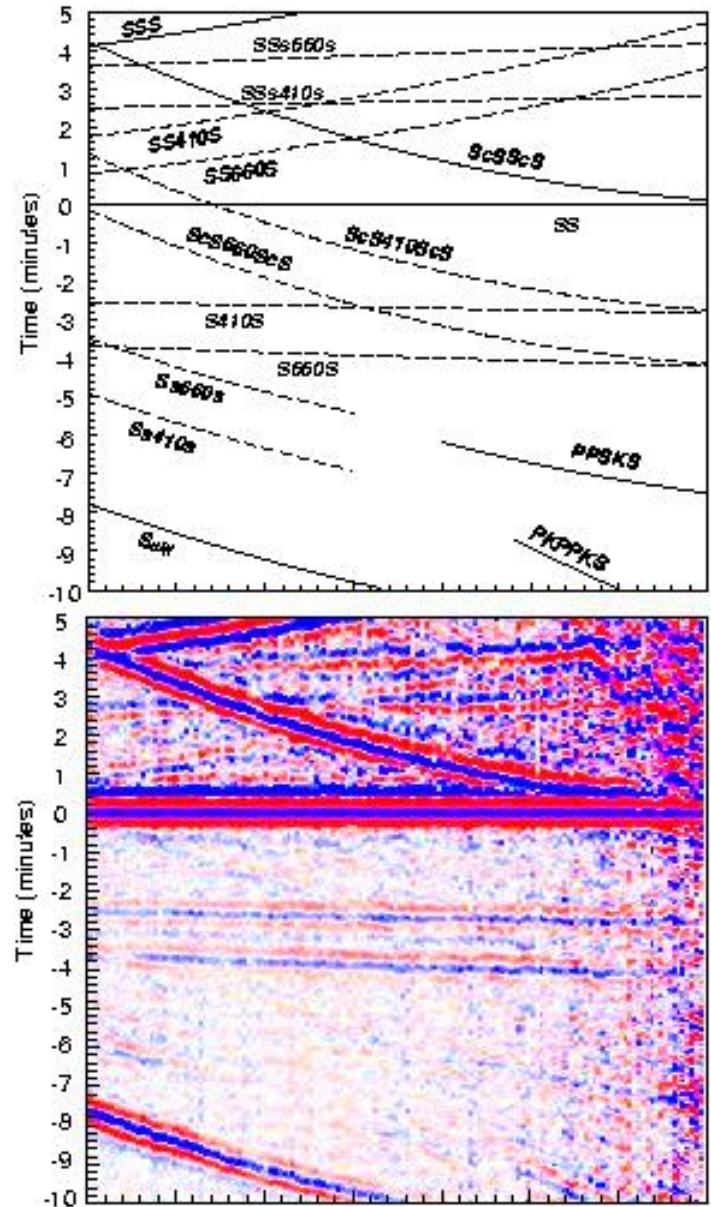
# Mantle 1-D seismic structure summary



- Between 410 and up to ~1000 km we are in the **MANTLE TRANSITION ZONE**
- A number of sharp discontinuities separate regions of high velocity gradients
- Main discontinuities are at **410** and **660** km.
- 660-discontinuity widely taken as the UPPER MANTLE/LOWER MANTLE boundary

# The transition zone

- Characterized by discontinuities in velocity and density models.
- Observed mainly by SS and PP underside reflections/



# The 410 discontinuity

Both velocities and density increase. Could be due to...

- Chemical change: Same minerals but with higher molecular weight (i.e. more Fe, less Mg)?
- Phase change: to a more densely packed structure?
- Or a combination of the above?

Major mantle component is olivine. What happens if it is subjected to P,T of transition zone?

- Experiments by Ringwood in the 1960s found that at about 12 GPa (400 km) and 1400C

Forsterite  $\rightarrow$  Beta  $\text{Mg}_2\text{SiO}_4$  (wadsleyite)

- Generally accepted as cause of the 410-discontinuity
- First observed naturally occurring in the Peace River Meteorite (Price et al 1983): formed during extra-terrestrial shock impact

Major mantle component is olivine. What happens if it is subjected to P,T of transition zone?

- Experiments at P,T expected for ~ 550 km  
Beta  $\text{Mg}_2\text{SiO}_4 \rightarrow$  Gamma- $\text{Mg}_2\text{SiO}_4$ (ringwoodite)
- ‘520’ seismic discontinuity is observed with stacking of certain large seismic datasets
- ‘520’-discontinuity corresponds to this phase change, or to other factors?

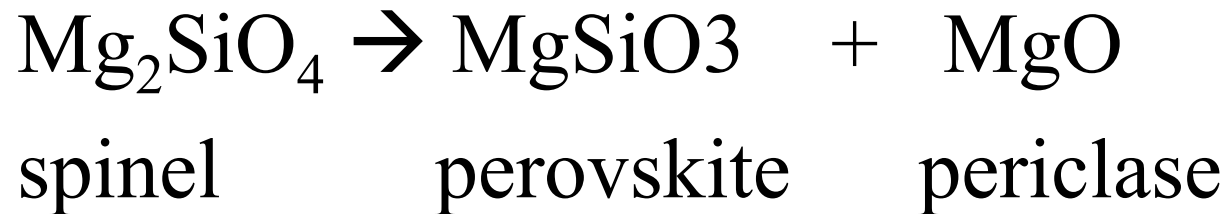
What about non-olivine component at transition zone P and T?

- $\text{MgSiO}_3$  undergoes a number of phase transitions in the P-T range of the transition zone  
pyroxene  $\rightarrow$  garnet (majorite)  $\pm$   $\rightarrow$  ilmenite
- Broad depth range of transition causes zone of high velocity gradients rather than single discontinuity



# The 660-discontinuity

- Much more difficult to simulate P,T conditions at 660 km than at 410, however...
- During 1970s and 1980s experiments indicated a further phase change in olivine component at 660 km



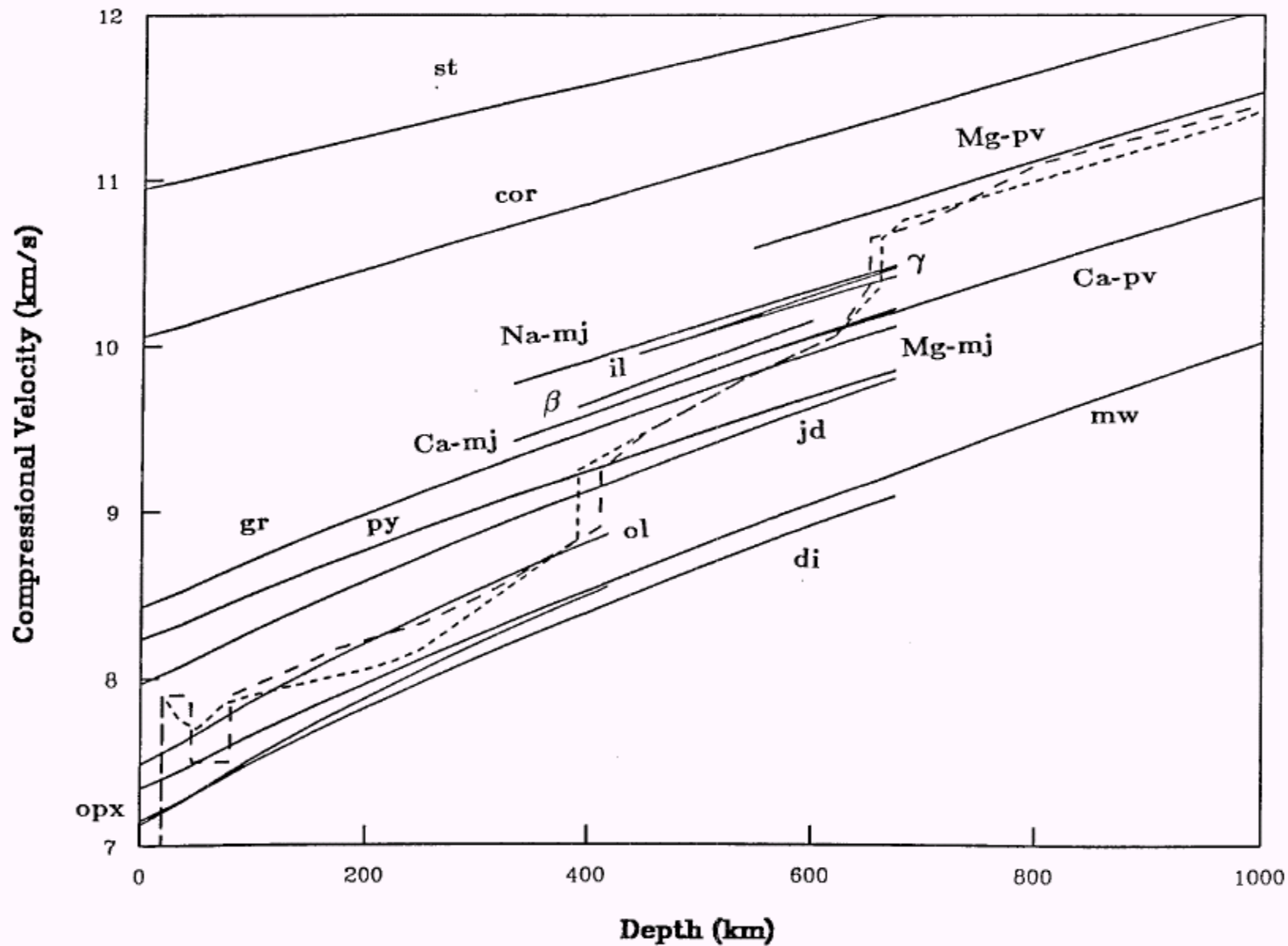


**FIGURE 3-7**

Calculated compressional velocity versus depth for various mantle minerals. "Majorite" (mj), "perovskite" (pv) and "ilmenite" (il) are structural, not mineralogical terms. The dashed lines are two recent representative seismic profiles (after Duffy and Anderson, 1988).

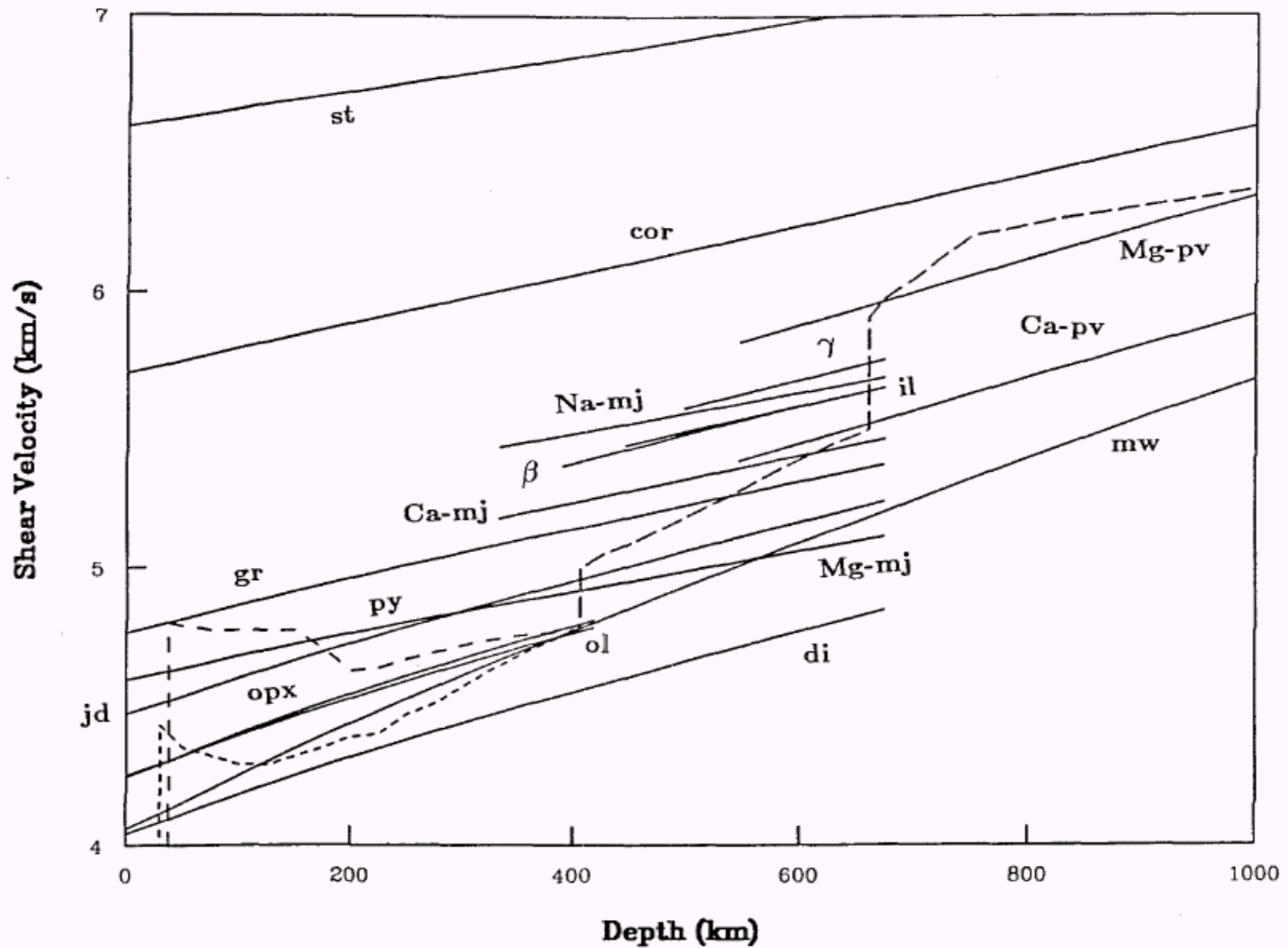


FIGURE 3-8

Same as Figure 3-7 but for the shear velocities (after Duffy and Anderson, 1988).

Is '660' discontinuity a chemical change as well as a phase change?

# Mineralogical models of the mantle

Cannot drill to mantle depths. Therefore we infer chemical composition and associated mineralogy from

- 1. Geochemistry
- 2. Laboratory experiments on possible mantle rocks at high P and T

# Mineralogical models of the upper 400 km

Pyrolite (Ringwood 1975) is a garnet  
peridotite mainly of olivine and  
orthopyroxene

Piclogite (Anderson and Bass 1984) is a  
clinopyroxene and garnet rich aggregate  
with some olivine

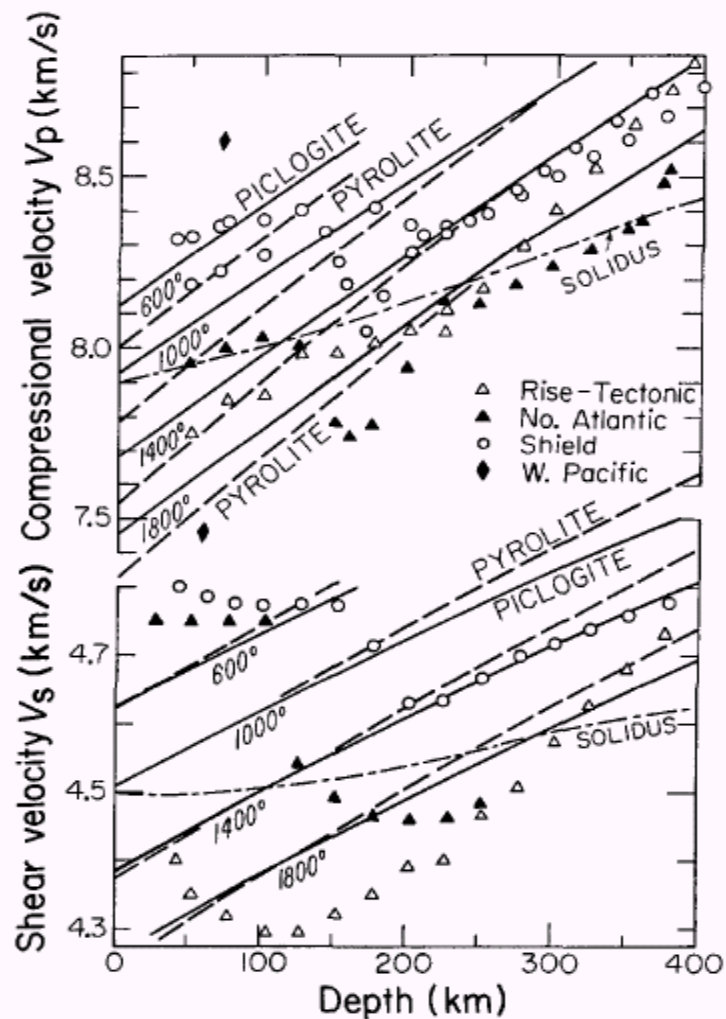
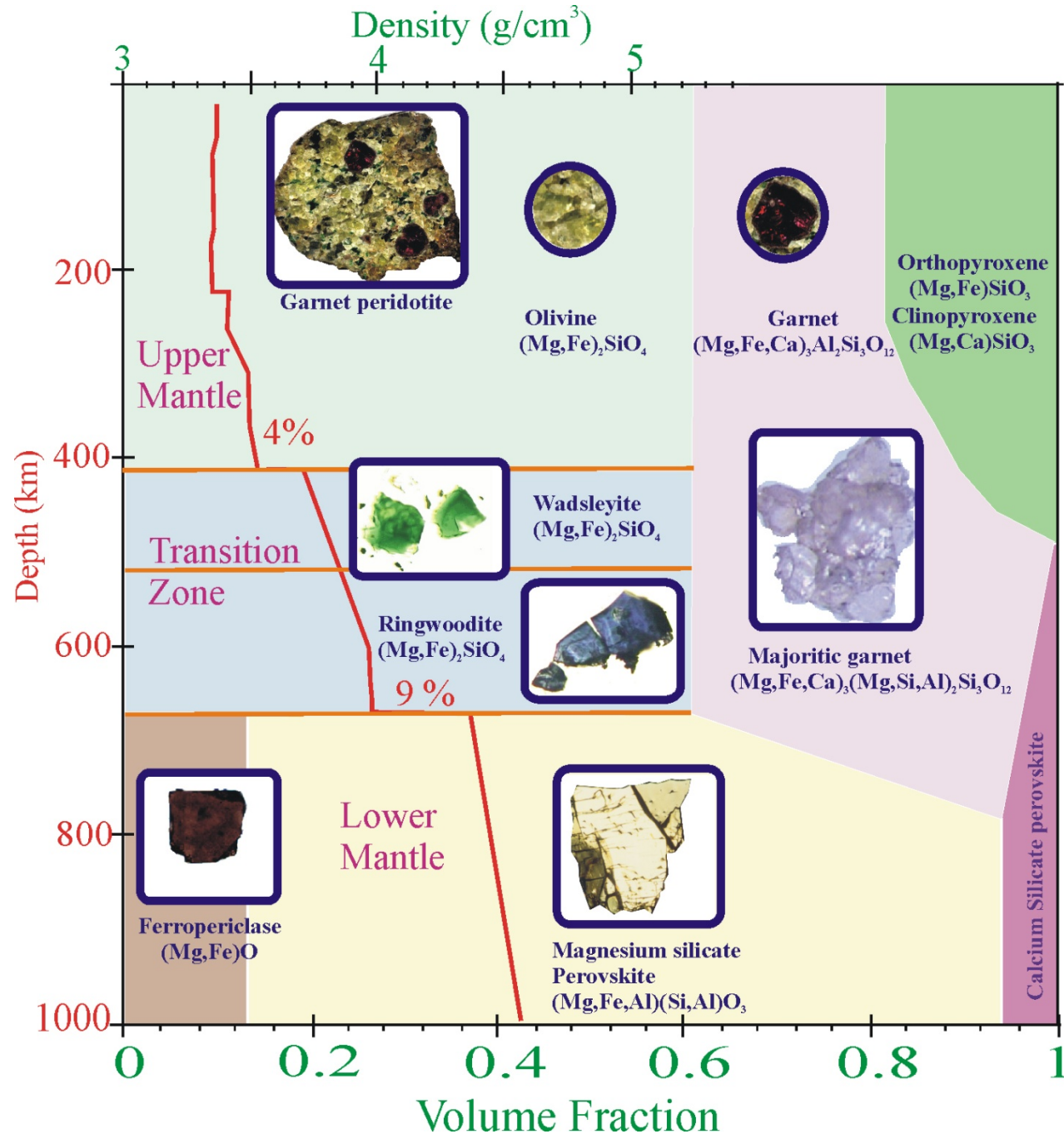


**FIGURE 3-5**

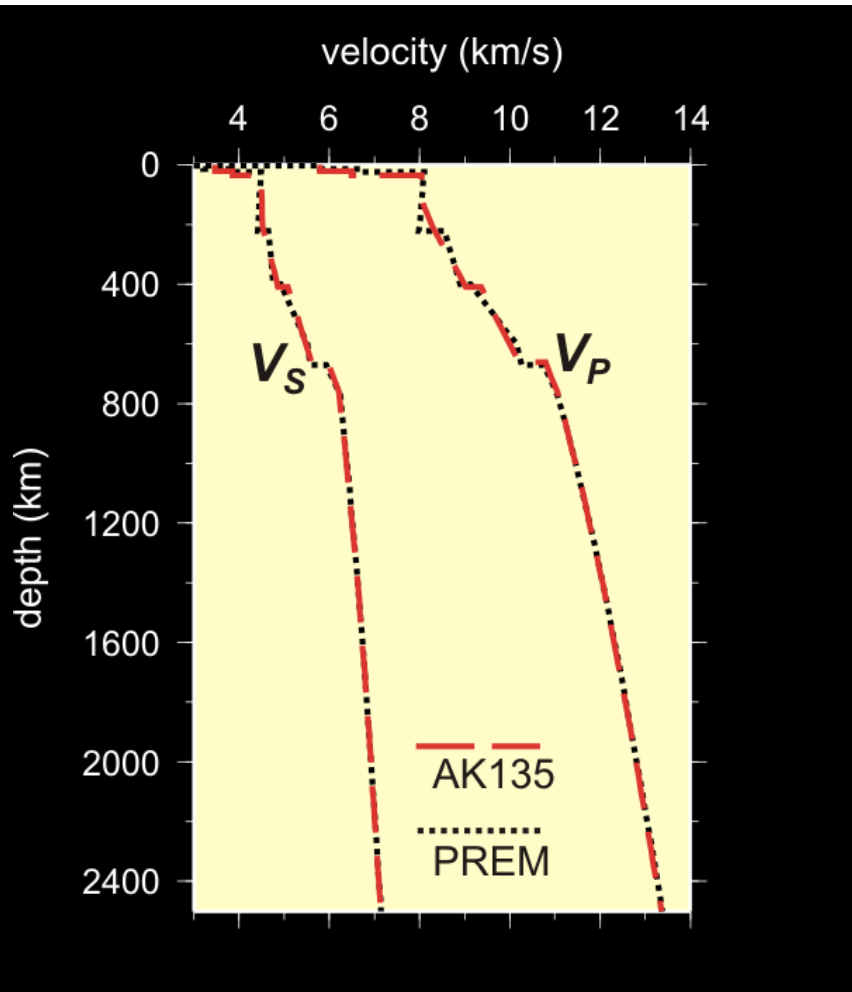
Compressional and shear velocities for two petrological models, pyrolite and piclogite, along various adiabats. The temperature ( $^{\circ}\text{C}$ ) are for zero pressure. The portions of the adiabats below the solidus curves are in the partial melt field. The seismic profiles are for two shields (Given and Helmberger, 1981; Walck, 1984), a tectonic-rise area (Grand and Helmberger, 1984a; Walck, 1984), and the North Atlantic (Grand and Helmberger, 1984b) region; two isolated points are Pacific Ocean data (Shimamura and others, 1977; after Anderson and Bass, 1984).

The lower mantle is relatively simple, except D''



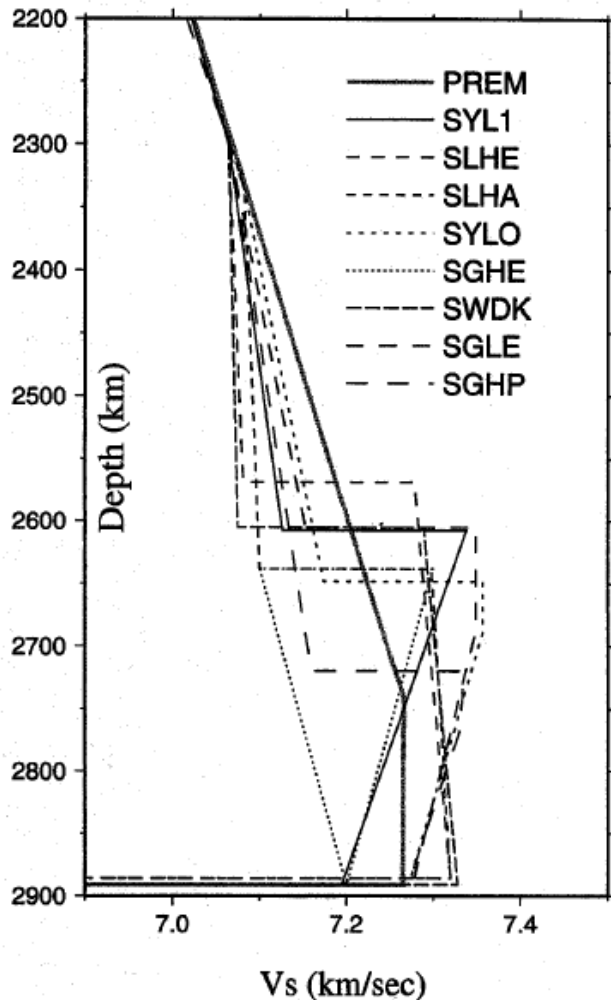


# Mantle 1-D seismic structure summary



- In the lower mantle, velocities increase smoothly and monotonically with depth, until  $\sim 2600$  km
- Between  $\sim 2600$  and  $2900$  km, have seismically complex D'' region

# D'' – seismically complex region in the bottom ~300 km of the mantle



- Reflectors / sharp discontinuity at top of D''
- Regionally varying S-wave anisotropy
- Ultra Low Velocity Zones
  
- Thermal boundary layer
- Perhaps melting
- Perhaps reaction zone (mantle-core)
- Perhaps slab 'graveyard'
- Perhaps origin of plumes

# Notion of MgSiO<sub>3</sub> perovskite stability

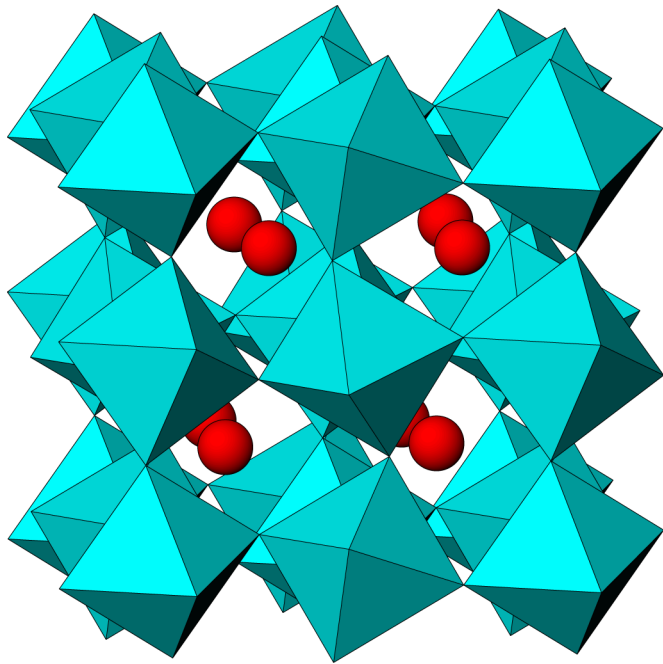
## Suggestions

- Orthorhombic (Mg,Fe)SiO<sub>3</sub> transforms to cubic or tetragonal symmetry
  - Decomposition into oxides in the mid-lower mantle
- Not confirmed by experiments or theoretical calculations

*Jackson and Rigden (1998): 'It seems most plausible that the orthorhombic Mg,Fe-perovskite phase remains stable relative to perovskites of higher symmetry along plausible geotherms throughout the lower mantle'*

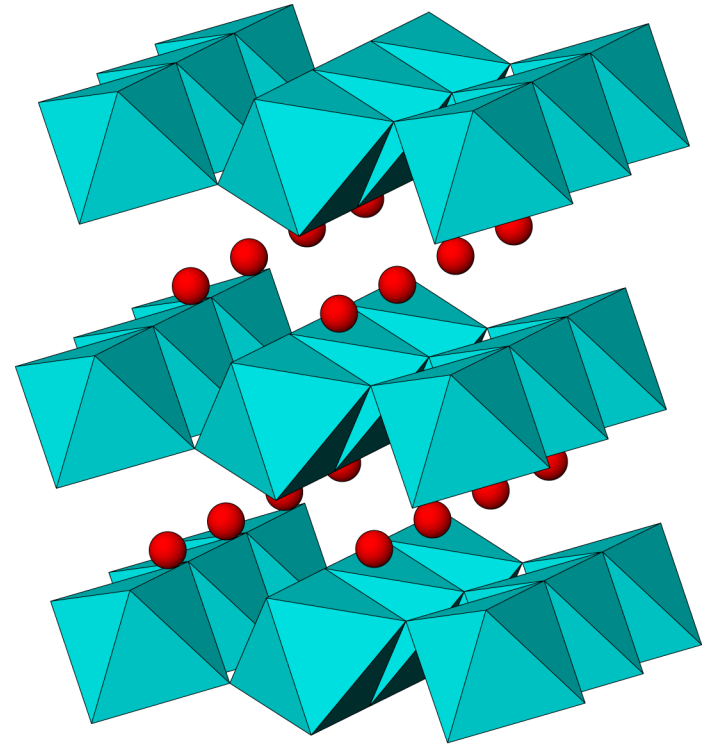
# 2004: Discovery of post-perovskite phase transition

- could explain some of the seismic properties of D''



by Dan Shim

perovskite  
(pv)



by Dan Shim

post-perovskite  
(ppv)

# The Core

## ***Geophysical observations....***

### DENSITY

- Average  $\rho$  of Earth =  $5.5 \text{ kg/m}^3$
- observed  $\rho$  surface rocks =  $2.7\text{-}3.3 \text{ kg/m}^3$

### MOMENT OF INERTIA

- I of Earth =  $0.33 MR^2$
- I for homogeneous sphere of constant  $\rho = 4 MR^2$

=> Mass is concentrated towards the Earth's centre

*Increasing rock density with depth due to compression alone?*

Adams-Williamson equation (Williamson and Adams, 1923)

$$\frac{d\rho}{dr} = -g\rho^2 K_s^{-1}$$

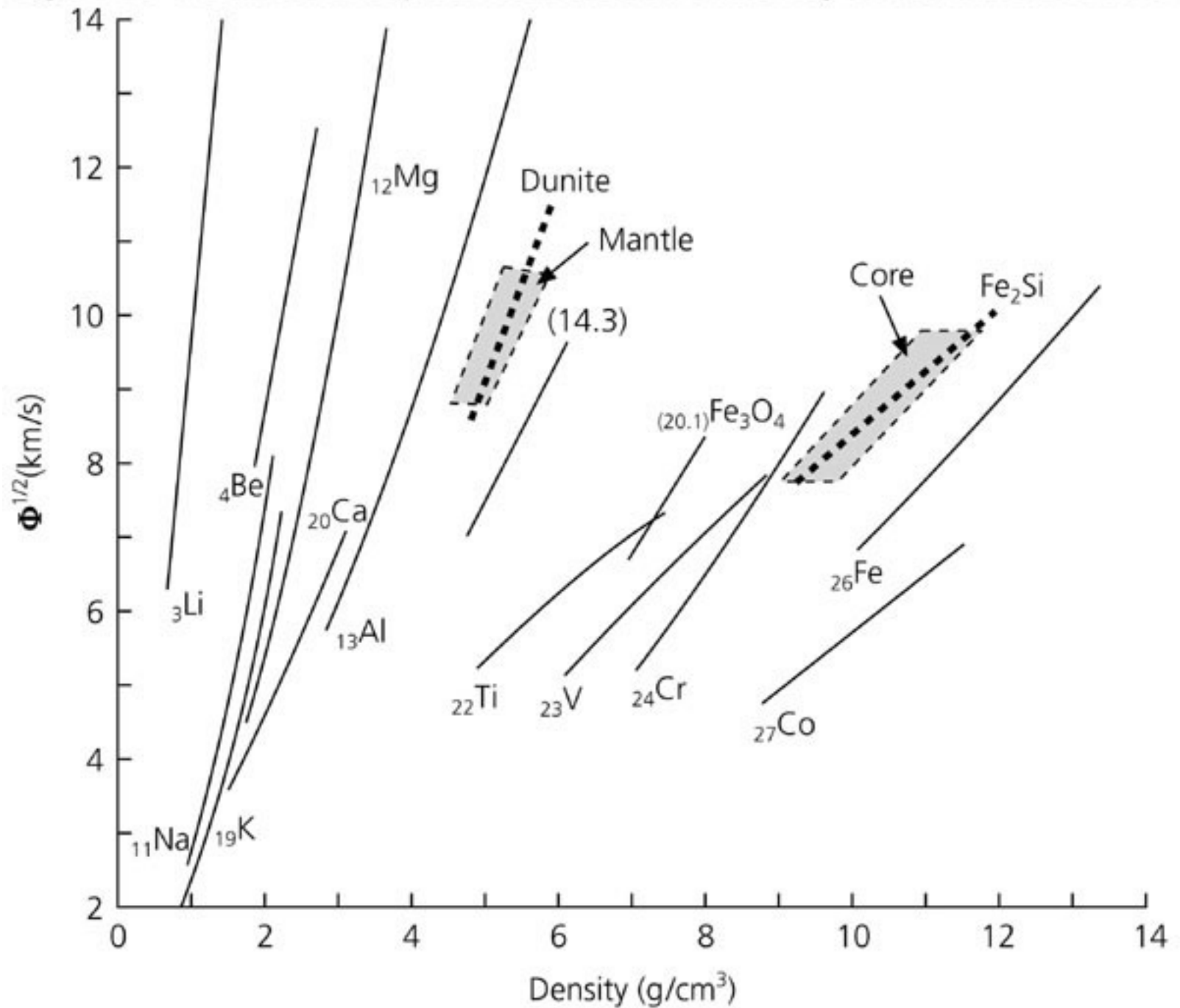
for a homogeneous, adiabatic material

Works for the lower mantle, but  $\rho$  does not increase fast enough to give  $\rho_{\text{ave}} = 5.5$

Williamson and Adams (1923) conclude that towards the centre of the Earth must be

*“...the presence of a heavier material, presumably some metal, which, to judge from its abundance in the Earth’s crust, in meteorites and in the Sun, is **probably iron**”*

**Figure 3.8-7: Bulk sound speed as a function of density for various materials.**





# The discovery of the core

- The core: Oldham 1906. Drop in velocity → shadow zone in P arrivals → liquid core
- Inner core: Lehman 1936. Increase in velocity → triplication → solid inner core
- Innermost core: 2003

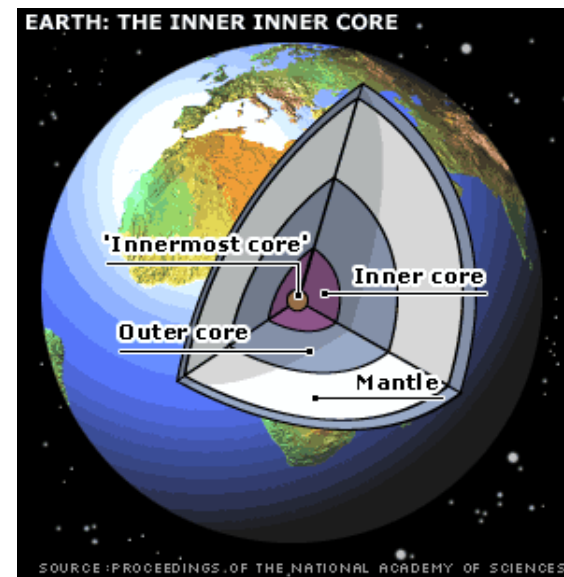


**Figure 3.5-7: Ray paths and travel times for major core phases.**

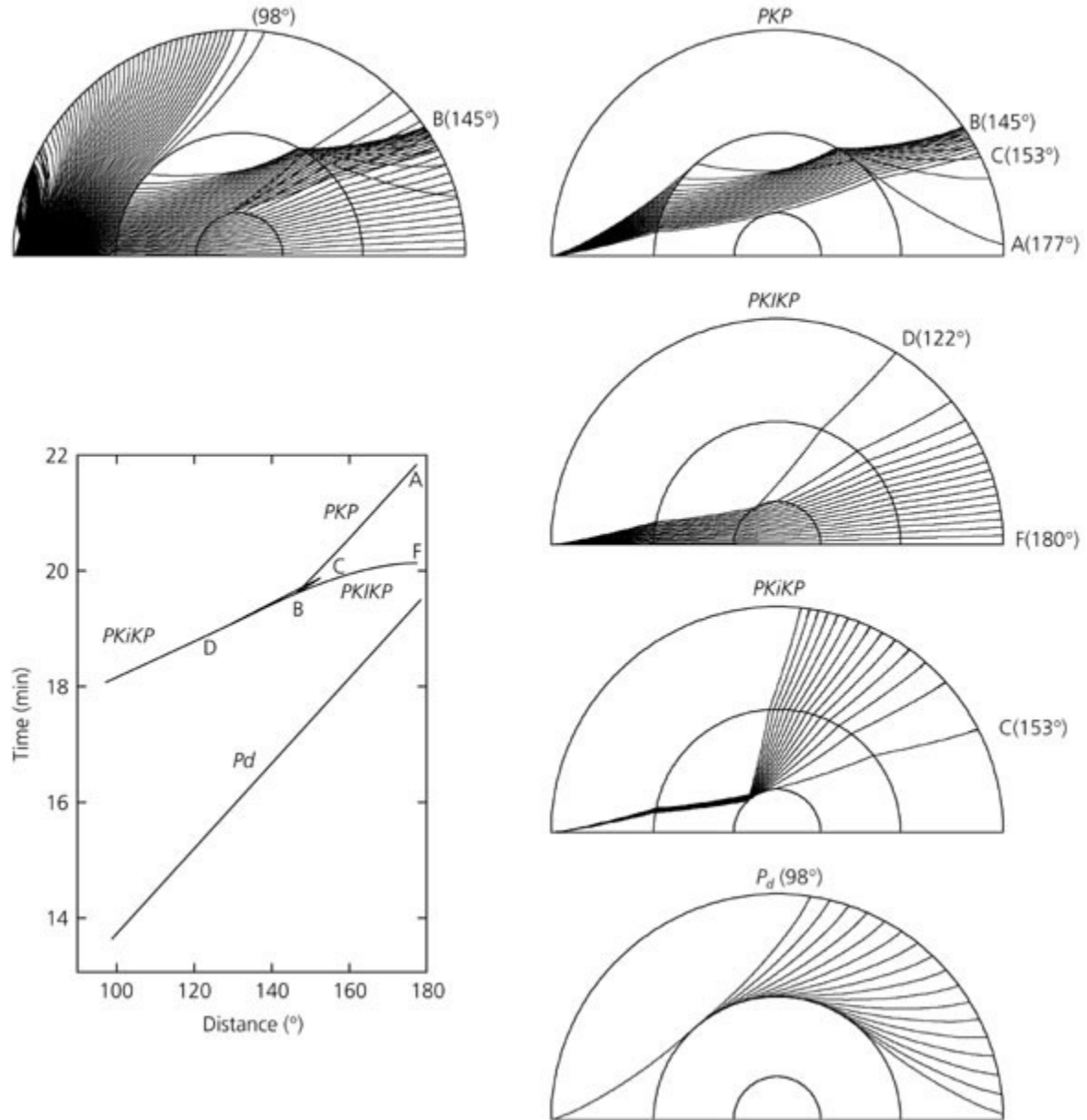


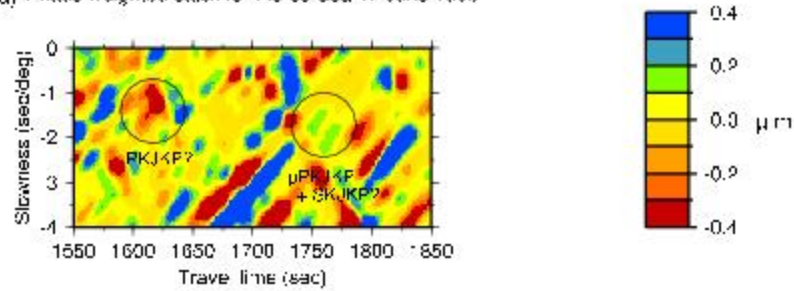
**Table 1** Observed Normal Modes of the Earth sensitive to the Structure of the Inner Core

Mode	Mean period (s)	No. of observations	s.e.m. (s)	UTD124B'—Solid inner core				UTD124B'—Liquid inner core		5.08M		HB <sub>1</sub>	
				Comp. period	Rel. error (%)	Inner core energy Compr.	Shear	Comp. period	Rel. error (%)	Comp. period	Rel. error (%)	Comp. period	Rel. error (%)
<sub>1</sub> S <sub>0</sub>	613.57	11	0.236	614.59	0.17	0.181	0.000	607.39	-1.02	610.06	-0.57	607.4	-1.01
<sub>2</sub> S <sub>0</sub>	398.54	40	0.084	397.59	-0.24	0.206	0.001	392.31	-1.59	391.42	-1.81	394.0	-1.14
<sub>3</sub> S <sub>0</sub>	305.84	7	0.129	306.00	0.05	0.233	0.003	301.36	-1.48	301.84	-1.31	300.9	-1.62
<sub>4</sub> S <sub>0</sub>	243.59	12	0.067	243.80	0.09	0.192	0.007	241.11	-1.03	241.55	-0.84	239.9	-1.51
<sub>2</sub> S <sub>2</sub>	904.23	21	0.487	904.43	0.02	0.001	0.080	914.94	1.17	917.80	1.50	915.1	1.20
<sub>5</sub> S <sub>2</sub>	397.36	11	0.157	397.03	-0.09	0.015	0.102	399.93	0.67	398.20	0.21	399.1	0.44
<sub>6</sub> S <sub>1</sub>	348.41	21	0.046	348.23	-0.05	0.068	0.011	347.10	-0.38	347.38	-0.30	346.6	-0.52
<sub>7</sub> S <sub>3</sub>	281.37	11	0.113	281.59	0.08	0.004	0.022	282.77	0.50	283.34	0.70	282.1	0.22
<sub>8</sub> S <sub>1</sub>	272.10	11	0.144	271.79	-0.11	0.115	0.052	271.00	-0.40	270.92	-0.43	270.5	-0.59
Nine modes—r.m.s.					0.12				1.01		1.00		1.02

### Figure (3)

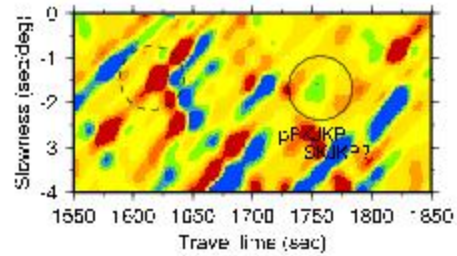
#### Observation

(a) Phase weighted stack for Flores Sea 17 June 1996

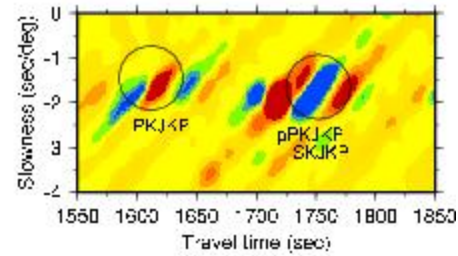


#### Modelling interpretation

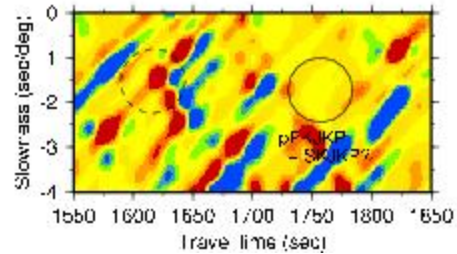
(b) Modes solid inner core



(d) Modes solid minus fluid inner core



(c) Modes fluid inner core



(e) WKB/L seismograms for J-phases

